Basic Reliability Tools for SHM protocols

Alain Bensoussan, Joseph Bernstein, Alain Bravaix

Reliability and Physics-of-Healthy in Mechatronics

Volume 15 – Reliability of Multiphysical Systems

Set by Abdelkhalak El Hami

(Book ISTE publishing Knowledge – Wiley)

Date: 18 October 2020

Bensoussan Alain
Dr.-Ing, Dr-HDR, IEEE senior member
Thales Alenia Space
Meta Competence Center
Toulouse, France
alain.bensoussan@thalesaleniaspace.com

Bernstein Joseph
Professor, IEEE senior member
Laboratory for Failure Analysis and Reliability of Electronic Systems
Ariel University
Ariel, Israel
josephbe@ariel.ac.il

Bravaix Alain
PhD, HDR, IEEE senior member
REER : Radiation Effects & Electrical Reliability, IM2NP, ISEN
ISEN Yncrea Mediterranée, Toulon, France
alain.bravaix@isen.fr

SUMMARY

Electronics components and devices, including equipment to systems, are fabricated from materials and structures that degrade with time under normal operational condition. It is necessary to anticipate and quantify system failure occurrence but the goal of "reliability engineering" is to clarify first the failure paradigm in term of statistics and Physics of Failure or simply Part Count approach. Many statistical approaches and underlying mathematics have been developed in the past decades of the last century to describe failure rates and the well-known bathtub curve showing a schematic of failure rate behavior with time.

From Wikipedia definition, *predictive (or logical) analysis encompasses a variety of techniques derived from statistics, data extraction and game theory that analyze past and present facts to make predictive assumptions about future events.*

In this applied reliability chapter, we would like to share our perception on the experimentally development applied on existing reliability and maintenance paradigms developed since decades by many authors and papers.

This Part I titled "Reliability Basic Tools for SHM protocols" aims to remind a) how applied engineering in predicting failure and monitoring SHM of electronic equipment and systems are implemented and b) to present basic statistic tools defined for reliability modelling implementation and studies related to active microelectronic parts. The second Part II is dedicated to the experimental application titled "Applied Engineering on Physics-of-Healthy and SHM on microelectronic equipment for aeronautic, space, automotive and transport operation" addressing how innovative technologies and Commercial-Off-The-Shelf (COTS) devices are pondered.

How to implement predicting failure and monitoring SHM of electronic equipment and systems?

High Temperature Operational Lifetest (HTOL) Standard is relatively poor to predict Mean-Time-To-Failure (MTTF) associated constant failure rate and reveals mostly ineffective for wearout modelling as no failure are observed. Furthermore, the MTTF50% is not a zero-failure guarantee (rather by definition is a 50% lot failure) and we should define rather a MTTF0.1% for high reliability application. At the same time, attention to long-life cycles on the part of manufacturers has nearly vanished due to the relatively overwhelming demand in the consumer market sector.

Three key questions are reviewed including a) How to apply reliability prediction tools to innovative technologies? b) What are the hypotheses made of and methodology implemented in these tools; and to what extent are they able to cover emerging technologies and applications? c) Prognostic Failure Model (PFM) what could be a proposed guideline to organize all concepts? We describe our approach in what is needed to answer these and other fundamental questions as for example:

The goal of reliability engineering is to anticipate and quantify failure occurrence but the science required is to clarify first the paradigm in term of statistics and Physics of Failure [1], [2] or Part Count failure approach [3] [4], [5]. Many questions are raised, and we try to address as listed here:

In term of Physics and Phenomenological Degradation:

What are the existing Standards, their advantages and drawbacks?

How to manage random and wearout failure rate model to implement predictive reliability and maintenance?

What role the "stressors" are playing?

How "indicators" are characterized and which criteria value to define?

How to deal with multiple stresses?

In very complex new technologies (less than 7 nm FinFET, GaN, Carbone NanoTube, …), what are the new failure mechanisms?

What if multiple failure mechanisms are coexisting? [5]

What is the impact on the accelerating factor (AF) in such complex mixed model (multiple stress, multiple failure mechanism)? [6]

How to apply reliability prediction tools to innovative technologies?

What are the hypotheses made of and methodology implemented in these tools; and to what extent are they able to cover emerging technologies and applications?

How to consider the effect of initial device quality, the influence of use and design options, the effect of mission profiles to model the Robustness [7] and the Reliability of complex systems and new technologies [8], [9], [10]?

In term of Application and experiments:

In very complex new technologies, observed failure mechanisms can often be accelerated simultaneously, causing a dilemma for reliability prediction.

In the domain of telecommunications, automotive, aerospace, satellite, military and the like, the need for accurate reliability prediction is as important as it ever has been. At the same time, attention to long-life cycles on the part of manufacturers has nearly vanished due to the relatively overwhelming demand in the consumer market sector.

How to explore field return and define optimized maintenance survey based on reliability prediction tools?

Assuming a qualification test experiment on 130 samples tested during 2000 hrs of 150°C HTOL with 0 failure observed.

What would be the device operating projected lifetime verified if the operational application is at T=45°C?

What should be the sample size and duration to demonstrate a Cumulative Density Function (CDF) equal of less than 0.1%

after 30 years in mission operation?

For Reliability prediction purpose do we need to consider Time-To-Failure for each failure mechanism either for a constant failure rate based on a Poisson statistic, or for wearout failure mechanism?

What would be the equivalent total λ_{total} and corresponding Time-To-Failure if all failure mechanisms are equally activated?

What the basic mathematics are?

Thermodynamics modeling established by S. Arrhenius (1896) [11], L. Boltzmann (1886) [12], then M. Evans and M. Polanyi in 1938 [13], E. Winner (1938) [14], S. Glasstone (1941) [15], G. Hammond (1955) [16], R. Drenick (1960) [17], E. Snow (1965) [18], N. Sedyakin (1966) [19], D. Cox (1972) [20] and periodically improved by H. Eyring et al. (1980) [21], J. McPherson (1999) [22] [23], or recently by E. Suhir (2013) [24] [25]. Modelling was supported by series of experimental papers from MIT (D. Jin and Del Alamo) [26], RAC Univ. of Maryland, University of Padova and G. Meneghesso's team [27], INTEL and IBM teams [28]. Since the break of 217^{+} standard, FIDES French group guideline is still in place and its next evolution is thought to consider non-constant failure rate model for predictive reliability. Not leaving aside main actors in this paradigm development we have to name most representative experts in the field which have influenced the written of these chapter J. Stathis, V. Huard, A. Bravaix, J. Bernstein, M. Meneghini, H. Zanoni, E. Wu and J. Sune, P.A. Tobias and D.C. Trindade, M. Nikulin and V. Couallier.

The paradigm of the Transition State Theory (TST) developed by E. Wigner in 1934 [14] and by M. Evans, M. Polanyi in 1938 [13] is an approach we can benefit too by adapting the concept of a unified semiconductor reliability model and multiple failure mechanisms related to Physics of degradation. Indeed in the early last century, the TST was applied to chemistry transformations by H. Eyring [21], and S. Glasstone et al. [15] in 1941. The TST was developed in chemistry based on the Hammond's postulate [16] published in 1955 applied to physical organic chemistry.

Multiple failure mechanisms and Physics of degradation in semiconductors may occur in a single set of time-to-failure data but without obvious points of inflection to help separate the mechanisms. J. McPherson in his book 3rd edition of Reliability Physics and Engineering provides the basics of reliability modelling [23], [22] recalled *generally, materials/devices exist in metastable states. These states are referred to as being metastable because they are only apparently stable. Metastable states will change/degrade with time. The rate of degradation of the materials (and eventual time-to-failure for the device) can be accelerated by an elevated stress (e.g., mechanical stress, electrical stress, electrochemical stress, etc.) and/or elevated temperature*.

Gibbs free energy diagram recalled in 3rd edition of J. McPherson book has provided the main inputs to describe multiple stressors environment effect including entangled accelerating factor picture as fully detailed in Part I. Numerical application for a study case on a FinFET technology assuming three major failure mechanisms defined by the following Arrhenius reliability parameters are also detailed.

These mathematics and physic approaches show how the activation energy is an Eyring model related to the stress and temperature applied and can no-longer be considered as a constant to extrapolate some experiment under high stress to nominal mission operation profile. That's the reason why several end-user Industries and Institutions are very cautious to perform lifetest conditions as close as the nominal conditions because of the change of activation energy attributed sometime wrongly to new (or different) failure mechanism while it is simply explained by the interaction of stress and temperature effect on the measured activation energy or to a best extend to Eyring law.

From these equations we can observe the **equivalent activation energy is dependent of the temperature T_0 and is increasing with temperature**. So, under the stress conditions, **the failure mechanism model is a non-uniform acceleration mechanism**.

The goal of Part I is to present basic statistic tools defined for reliability modelling implementation and studies related to active microelectronic parts (Integrated circuits, power transistors, etc) when exploited in operational environment for long term high reliability application.

Basics mathematics on serie-parallel systems reliability are presented with some approximation considerations for distribution queues statistics.

Conclusion and perspective open the door for the next Part II related to Predictive Reliability supported by experimental and Physics of Failure (PoF) or what we call Physics of Healthy (PoH).

Physics of degradation in semiconductors may occur in a single set of time-to-failure data but without obvious points of inflection to help separating the mechanisms. In his book, J. McPherson titled "Reliability Physics and Engineering provides the basics of reliability modelling" [23], [22] stated "*generally, materials/devices exist in metastable states. These states are referred to as being metastable because they are only apparently stable. Metastable states will change/degrade with time. The rate of degradation of the materials (and eventual time-to-failure for the device) can be accelerated by an elevated stress (e.g., mechanical stress, electrical stress, electrochemical stress, etc.) and/or elevated temperature"*.

Part II goal is to concentrate on experiment supported by models and field return showing the "true life" observing simultaneous stress environment (various mission profiles) and multiple failure mechanisms.

Keywords— Probabilistic Design-for-Reliability, SHM, Reliability, PoF, PoH, Transition State Theory, Statistics, Semiconductors, Wide Band Gap, Deep Sub-micron, FinFET.

NOTATION

BAZ	Boltzmann-Arrhenius-Zhurkov
BEOL	Back End Off Line
BTI	Bias Instability (NBTI or PBTI)
CA	Constructional Analysis
CCC (or CC)	Channel Cold Carrier
CDF CFET	Cumulative Distribution Complementary Transistors Function
CHC or HC)	Channel Hot Carrier
DIBL	Drain-Induced Barrier Lowering
DoE	Design of Experiment
DSM	Deep-Submicron technology
$c(x_i)$	Energy factor related to stress parameter x_i
E_a	Activation energy
$E_{a\_effective}$ or E_{aa}	effective activation energy related to multiple stress reliability test sequence
EES	Electron-electron scattering
ECSS	European Cooperation on Space Standardization
EMC	Electromagnetic compatibility
EM	Electromigration
ESD	ElectroStatic Discharge
EOS	Electrical Overstress
EOT	Equivalent Oxid Thickness
EVD	Extreme Value Distribution
$\in$ or $\in(t)$	Gibbs Free Energy for a device
FEOL	Front End Off Line
FF	FinFET
FI	Fan In
FO	Fan Out
FRAME	Failure Risk Analysis Methodology
GaAs	Gallium Arsenide
GaN	Gallium Nitride
G	Gibbs Free energy
GIDL	Gate-Induced Drain Leakage
γ_i	Stress factor as percentage of burnout limits for label i as current *I*, voltage *V*, P_{DC} power, P_{in} signal input power
HBD	Hard breakdown
HCD	Hot carrier degradation
HCI	Hot carrier injection mechanism
I_{BO}	Current burnout limit value
I_{G_leak}	Gate leakage current between gate and source at V_{GS} and V_{DS}
I_{G_LBO}	Gate leakage current between gate and source at high V_{GS} and V_{DS} close to burnout or breakdown.
I_g	peak gate current during stressing
I_{HCG}	Current due to hot carrier generation
ILD	Inter-layer dielectric
I_{sub}	peak substrate current during stressing
$\lambda(t)$ or *IFR*	Instantaneous Failure Rate or Hazard function
k	Boltzmann's constant ($1.3807 \cdot 10^{-23}$ J/°K or $8.6174\ 10^{-5}$ eV/°K).
MESFET	Metal-semiconductor field effect transistor
MR	Maximum rating
M-STORM	*M*ulti-phy*S*ics mul*T*i-stress*O*rs predictive *R*eliability *M*odel
M-TOL	Multiple Temperature Overstress life-test
MVE	Multi-Vibrational Excitation
NAF	NMOS Acceleration time Factor
NBTI	Negative bias temperature instability
NTF	DC NMOS Acceleration Time Factor
PAF	PMOS Acceleration Factor
PBTI	Positive bias temperature instability
P_{BO}	Power burnout limit value
PDF	Probability Density Function
PDfR	Probabilistic Design-for-Reliability
PHEMT	Pseudomorphic High Electron Mobility Transistor
PMOS	P type Metal Oxide Semiconductor
PoF	Physics of Failure
PoS	Physics of Stress
P_q	Poisson statistic function
q	Number of failures in Poison statistic function
QBD	Charge at breakdown
SBD	Soft breakdown
S_e	electrical indicator or signature of the failure mechanism
S_i	Stress parameter for i as current *I*, voltage *V* or P_{DC} power consumption or P_{in} signal input power
S_{iBO}	Stress parameter at burnout limit value
SiC	Silicon Carbide
SM/SV	Stress migration/voiding
SOA	Safe Operating Area
SVE	Single Vibrational Excitation
TDDB	Time Dependent Dielectric Breakdown
TST	Transition State Theory
TSRM	Transition State Reliability Model

CONTENT

Chapter I: Basic Reliability Tools for SHM protocols

Bensoussan Alain
Dr. Ing., Dr.- HDR, IEEE senior member
Thales Alenia Space
Meta Competence Center
Toulouse, France
alain.bensoussan@thalesaleniaspace.com

Bernstein Joseph
Professor, IEEE senior member
Laboratory for Failure Analysis and Reliability of Electronic Systems
Ariel University
Ariel, Israel
josephbe@ariel.ac.il

Bravaix Alain
PhD, HDR, IEEE senior member
REER : Radiation Effects & Electrical Reliability, IM2NP, ISEN
ISEN Yncrea Mediterranée, Toulon, France
alain.bravaix@isen.fr

"As long as mathematical laws refer to reality, they are not absolute, and as long as they are absolute, they do not refer to reality"

"Tant que les lois mathématiques renvoient à la réalité, elles ne sont pas absolues, et tant qu'elles sont absolues, elles ne renvoient pas à la réalité."

Discours à l'Académie Scientifique de Prusse, Janvier 1921. Albert Einstein

I. Introduction

Trending articles and news related to the semiconductor industry are published in various web sites. In a paper signed by Khaveen Jeyaratnam, a specialist in financial analysis, valuation and investment research presented the Semiconductor Industry Value Chain and discussed the Top 3 Semiconductor Foundries In The World in March 21, 2019 (https://seekingalpha.com/article/4250209-top-3-semiconductor-foundries-world). He highlights "*the semiconductor industry is experiencing heavy growth in demand from the onset of the fourth wave of technology which includes robotics, artificial intelligence, nanotechnology, quantum computing, biotechnology, the Internet of Things, fifth-generation wireless technologies (5G), augmented/virtual reality, 3D printing, and autonomous vehicles.*"

The top 4 worldwide semiconductor foundries by revenue for 1H18 are TSMC (56.1% market share), GlobalFoundries (9.0%), UMC (8.9%), and Samsung (7.4%). Currently TSMC ($32B+) is the number one foundry by a very large margin with GF ($6B+), UMC (>$5B+), Samsung (>$5B+), and SMIC $3B+) barely visible in the rearview mirror. In Semiwiki web site it was mentioned the full year 2018 revenues of TSMC, by technologies represent 9% for the 7-nanometer node size (25% in 2019), 11% for the 10-nanometer, 23% for the 16/20-nanometer, and 63% for the 28-nanometer and below. On the other side, GlobalFoundries offer CMOS, FinFET and FD-SOI technologies.

Electronics components are made from devices, including equipment to complete systems, are fabricated from materials and structures that degrade with time under normal operational condition. This is a fundamental consequence of the second law of thermodynamics which cannot be avoided in our physical world. We cannot afford uncertainty of systems based on various domains including Aeronautics, More Electrical Aircraft, Space, Automotive and autonomous vehicles relying on hundreds, thousands and millions of electronic devices per vehicle and employing fleets of thousands. Degradation has been observed also, to depend on many environment parameters, both intrinsic and extrinsic, as follow due to:

- Packaging and component manufacturing and process distributions
- Original material and geometry arrangement into devices
- Internal and external environment conditions named "***stressors***" so as biasing (voltage, current, power dissipation, transient, signal level), temperature (low, high, constant, variable), irradiation levels (particles, X-ray, γ-ray), humidity, other pollution gases, etc [23], [5],

We can model failure rates and degradation, assuming independently thermal activation processes and at random, until some critical device parameter can no longer meet the required specification for proper device or system functionality. Some parameters (considered as electrical signatures) can be identified as **precursor** of failure occurrence. So, the failure is really defined when a specific functional parameter is "enough" affected to create a malfunction of the system. The threshold, for an indicator degradation leading to a final system parametric failure or a catastrophic failure depends on the stressor intensities (level of stresses with respect to the intrinsic limits supported by a device) and time.

Many statistics and mathematics have been developed over the centuries [11], [12], [13], [21], [23], [29] to describe failure rates and the well-known bathtub curve showing a schematic of failure rate behavior with time. In this approach three domains were traditionally established: Infant Mortality, Random failure and Wearout Failure [2], [30], [31]. The common "Time-to-Failure" parameter (TTF) e.g. the time for a given population to survive, to have its number of "good" elements be ½ the original population [23].

This simplified viewpoint which has drawbacks and suffers from some vagueness in the definition of failure when considering innovative commercial-off-the-shelf (COTS) devices use (Deep Sub-Micron technology node size lower than 20 nm [32] or Wide Band Gap semiconductor based devices [33]):

- Infant mortality, random failures and wearout are generally based on catastrophic failures observations in the field. When considering parametric failures this may induce different interpretation and results [6] [34], [35].
- Temperature definition is a key parameter which can modify the interpretation and the reading of results [3], [36]: for example temperature can be considered as ambient or case or junction.
- Failure criteria definition is observed to be a sensitive parameter impacting the TTF [37], [38], [39].

Saying this, broad application of disruptive technologies in embedded Hi-Rel systems requires all reliability aspects to be modeled and quantified in order to predict TTF and wearout Remaining Useful Life (RUL) both impacted by mission profile of electronic systems.

This chapter will first detail the existing models, tools and methodologies existing for COTS new emerging technologies. We will see why and how the concept of activation energy is an Eyring model related to the stress and temperature applied and the use of an approximated constant activation energy can no-longer be considered as a constant to extrapolate some experiment under high stress to nominal mission operation profile.

We will present hypotheses, baselines and definitions of reliability parameters through the prism of Transition State Theory (TST) in order to show how the multi-dimensional stress environment can be simply modelled. Reliability prediction is then

supported by the extrapolation of lifetime models based on what we call, Physics of Healthy (PoH). PoH in term of reliability prediction is the calculation of the statistical failure probability described by physics-based rate processes. The methodology presented here is a direct application of the well-known, standard, proportional sum-of-failure-rates where the rates are calculated by thermodynamically determined statistical processes.

A section will address the Transition State Reliability Model and reliability Physics of Healthy defined as the probability of a product performing it intended function for a given amount of time and mission profile. Basic approaches are recalled so that engineering designs and materials are detailed to construct reliability tools as defined by conventional reliability standards.

A last section will focus on system reliability (series and parallel) mathematic recalls and proposed approximations through four Lemmas.

L1: A series system constituted of *n* identical and independent elements, each described by a POISSON distribution (λ_0) reliability model can be approximated by a general equivalent POISSON distribution with parameter $n \cdot \lambda_0$.

L2: A parallel system constituted of *n* identical and independent elements, each described by a POISSON distribution (λ) reliability model can be approximated by a general equivalent WEIBULL distribution with parameters λ and $\beta = n$ with an error lower than 1% for time operation lower than 30%· MTTF for the example shown.

L3: A parallel system constituted of *n* identical and independent elements, each described by a reliability WEIBULL distribution (α, β) model can be approximated by a general equivalent WEIBULL distribution with parameter (α, $\beta \cdot n$) with an error lower than 1% for time operation lower than 75%· MTTF.

L4: In a series-parallel system constituted of *n* identical and independent elements, each described by a reliability POISSON distribution (λ), its reliability model can be approximated by a general equivalent WEIBULL distribution with parameter (θ, β= m) with an error lower than 3% for time operation lower than 50%· MTTF.

The fact that microelectronic devices are manufactured in such large quantities with established variability, deviations (fluctuations) and uncertainties make them the quintessential framework through which all reliability prediction and evaluation should be understood. Existing reliability models may sometimes be less accurate for emerging and non-mature technologies because of lack of customer and user's feedbacks due to the short product life cycle. The consumer market relies on short life cycles. Consequently, the very nature of the electronics industry, where so many parts having so many interacting physical phenomena, electrical performances, geometrical and material parameters, and application design conditions makes them the ideal example for reliability evaluation that can be applied to any other product or industry.

This chapter Part I will prepare the foundation to answer three central questions:

1. How to apply reliability prediction tools for innovative technologies?
2. What are the hypotheses made of and methodology implemented in these tools; and to what extent are they able to cover emerging technologies and applications?
3. Prognostic Failure Model (PFM): what could be a proposed guideline to organize all concepts described?

A. *COTS and Emerging technologies in Deep-Sub-Micron technologies: short overview*

In a recent synthetic paper published on SemiWiki on LithoVision 2019 – Semiconductor Technology Trends and their impact on Lithography, Scotten Jones [40] presented highlights on NAND scaling with layers, DRAM peripheral scaling and Logic high performance and IoT. Evidence is shown on the complexity of market push technology in the 3D NAND mask counts and bit density trends. "The transition from 2D NAND to 3D is enabling the continuation in bit density scaling by using the third dimension (see **Figure II-1**). DRAM scaling is limited by capacitor size and facing physical limits. Logic is continuing to scale but fundamental limits on 2D shrinks are looming. Leading edge logic has evolved from planar transistors to a split roadmap with FinFET for high performance and things like FDSOI for IOT. Longer term gate-all-around is on the horizon."

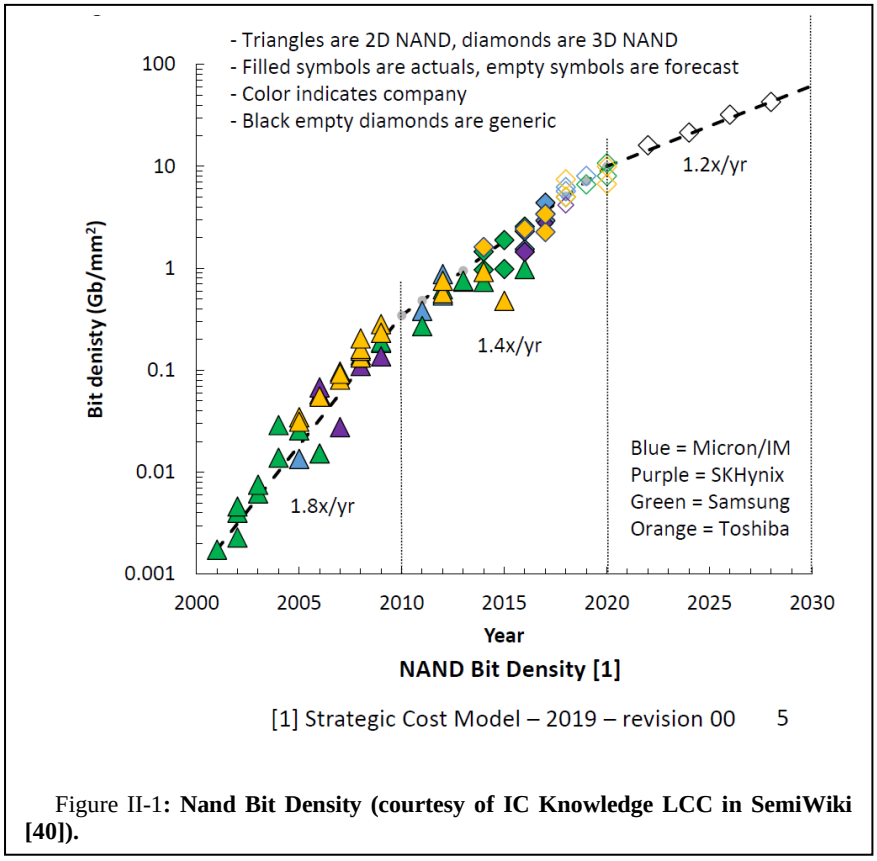

Figure II-1**: Nand Bit Density (courtesy of IC Knowledge LCC in SemiWiki [40]).**

From **Figure II-2** extracted from ref [40] we can see that for planar transistors the effective gate width (Weff) was defined by the transistor gate width. For FINFETs the Weff depends on the width and 2x the height of the fin and therefore Weff can only be varied in discrete increments. With GAA the Weff is 2x thickness and 2X width.

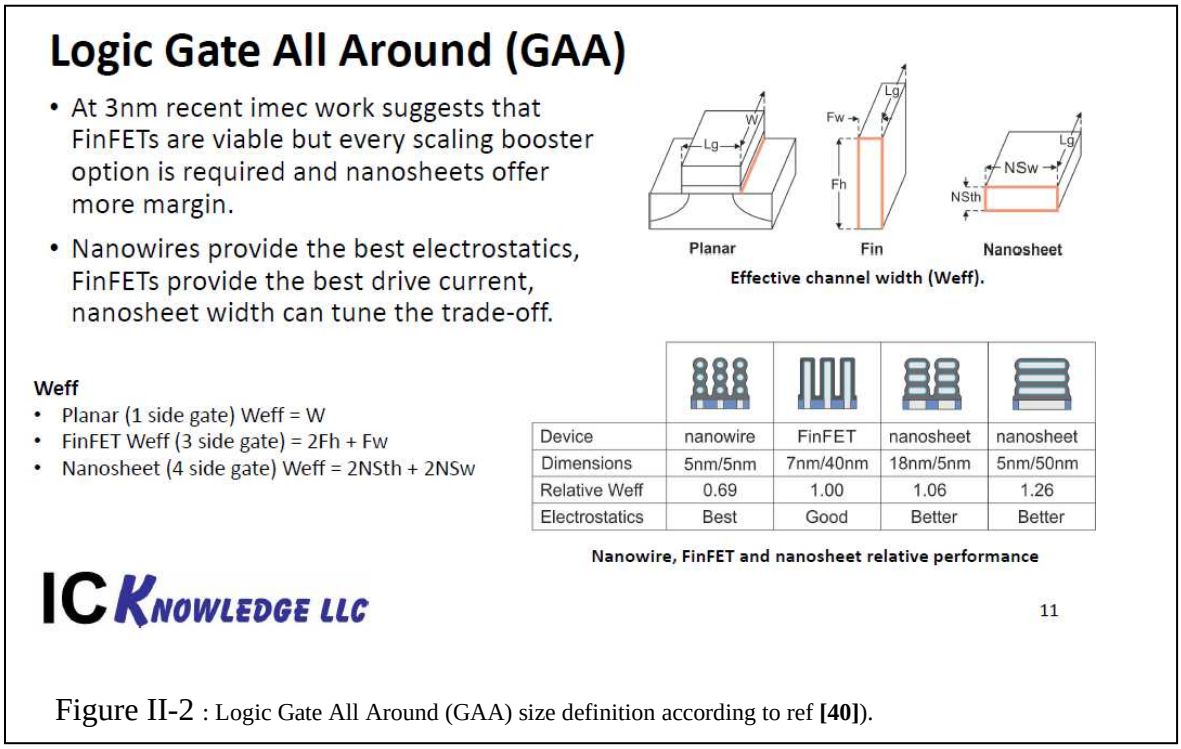

Figure II-2 : Logic Gate All Around (GAA) size definition according to ref **[40]**).

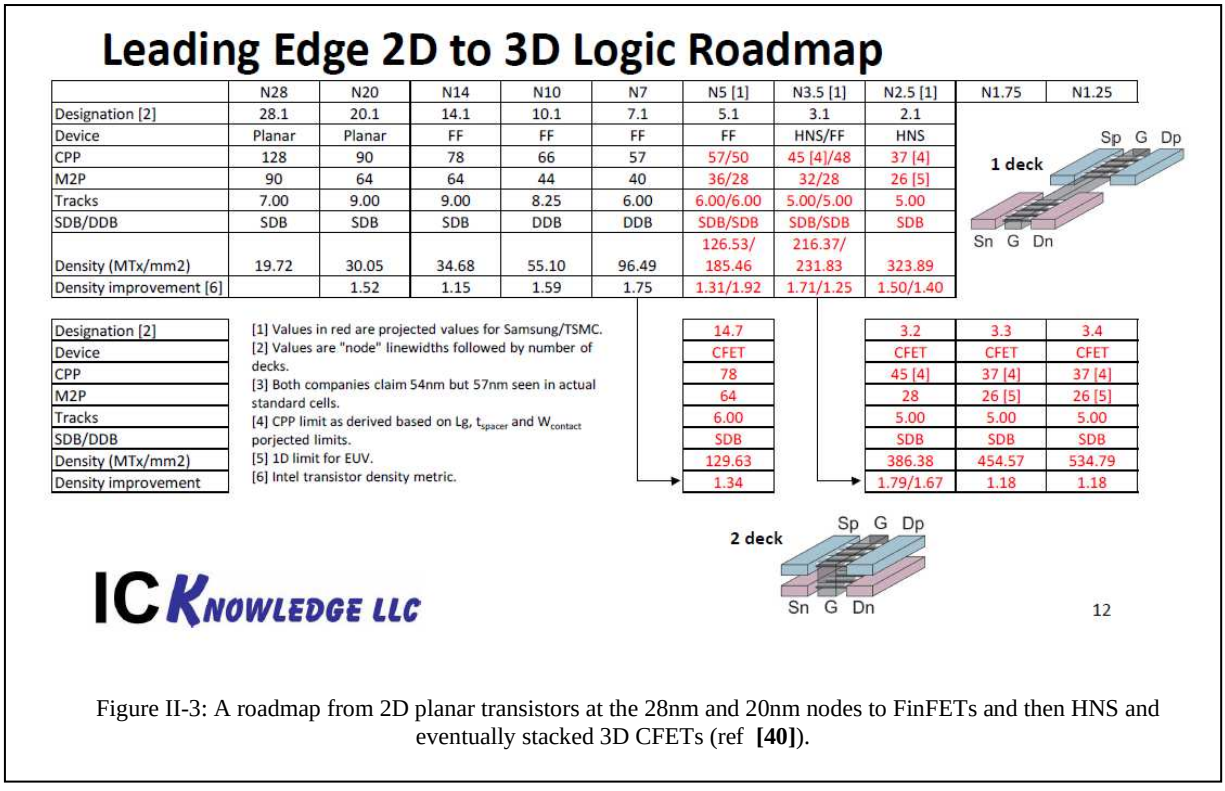

Figure II-3: A roadmap from 2D planar transistors at the 28nm and 20nm nodes to FinFETs and then HNS and eventually stacked 3D CFETs (ref **[40]**).

From **Figure II-3**, for Node 5 (N5) and N3.5 we have specific projections for Samsung and TSMC. At N2.5 we have a generic forecast with both companies converged on HNS.

For 3D we have options beginning with a relaxed 14nm design rule CFET with 7 layers as well as more lithographically aggressive 3.2, 3.3 and 3.4 Complementary Transistors (CFETs) with 3nm lithography and 2, 3 and 4 layers. The pictures show an nFET and pFET side by side for a single layer device and then a pFET over and nFET for a 2 layer CFET.

According to Scotten Jones it is shown how the EUV helps to mitigate mask count increases and about 60 to 70 mask sets. CFET at a 1.75nm node also helps to control the lithographic difficulty by being highly self-aligned.

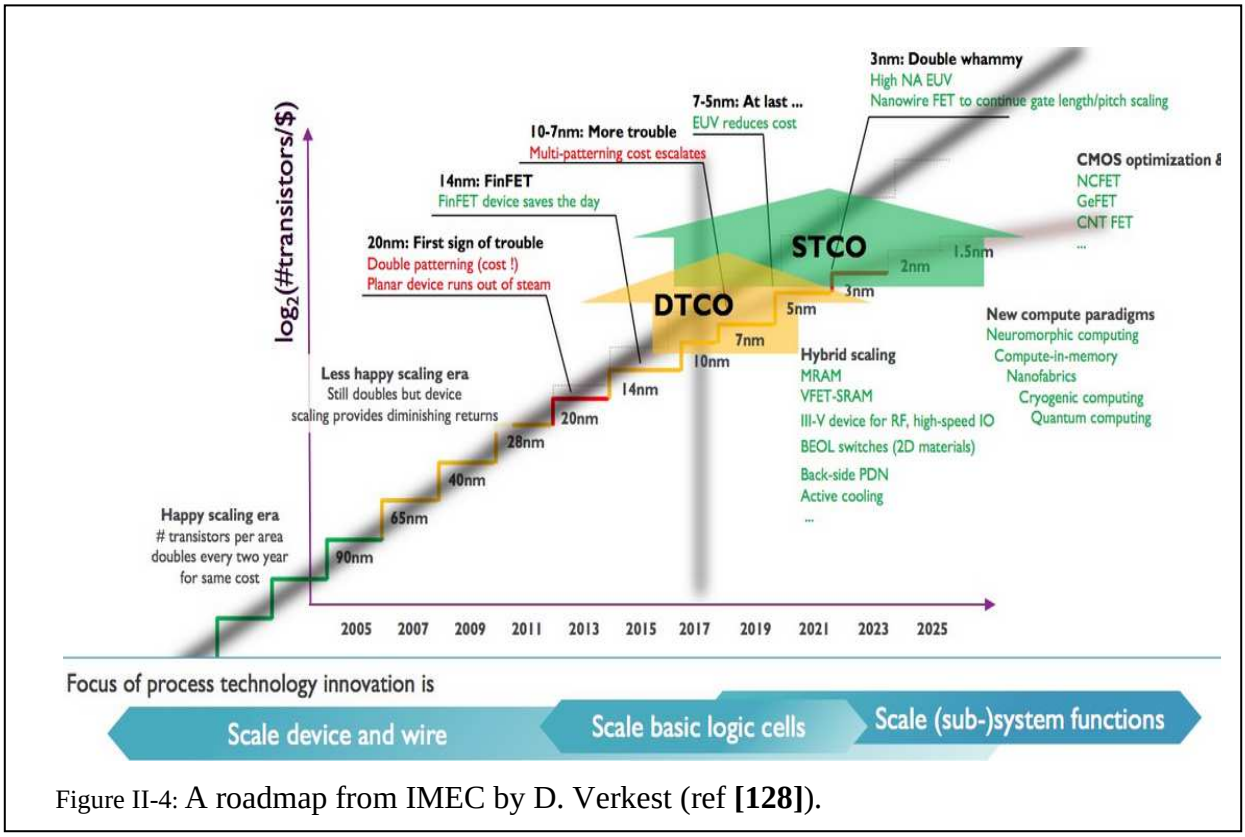

Figure II-4: A roadmap from IMEC by D. Verkest (ref **[128]**).

Traditional device scaling continues but dimensional scaling impacts performance too as shown in Figure III.4 an extract from Cadence blog Paul McLellan published in June 2018. “Fundamental new devices such as carbon nanotubes or 3D materials are still far from maturity. So there have been three eras. In the first, the focus was to scale the devices and wires. In the second, the focus was reducing the size of basic logic cells (and the SRAM cell). In the future, the focus has to move to scaling entire sub-system functions.”

In another internet link title “Big Trouble at 3nm” published by Mark Lapedus, Executive Editor for manufacturing at Semiconductor Engineering, in June 21st, 2018 [41], reports Dan Mocuta (director of logic integration and devices at Imec) words : “the key element is variable widths. You can control it better than the variable height of a fin,”.

“In a finFET technology, the width of the device is quantized. You can have one fin, two fins, three fins or whatever. In nanosheets (see Figure II-4 and Figure II-5), you have a fixed number of nanosheets on top of each other. But you can play with the width. Now, you have access to a continuum of device widths, which you didn’t have for the finFET,” Mocuta said. “For example, you want to have an area that drives a lot of current. That could be a buffer. Then, you want to have an SRAM with a very small footprint. There are different needs on the chip that can be met.”

Nanosheets are promising, but that isn’t the only option. With a breakthrough, finFETs could extend beyond 5nm. Another option is to wait until the industry develops a better transistor. Still another way is to get the benefits of scaling by putting multiple devices in an advanced package.

For now, gate-all-around technology appears to be the most practical technology after finFETs.

Modeling such novel transistors to establishing reliability figures for risk assessment is tremendously challenging. Market will be driven by system application and Deep Sub Micron technology as a “COTS integration plug and play” will require to implement risk assessment methodology to satisfy market related to Automotive, Aeronautic, and Space where system failures in normal operation and harsh mission profile condition are strictly forbidden for some period of time. Not clearly yet addressing the next question related to MTTF or MTBF for system repairs.

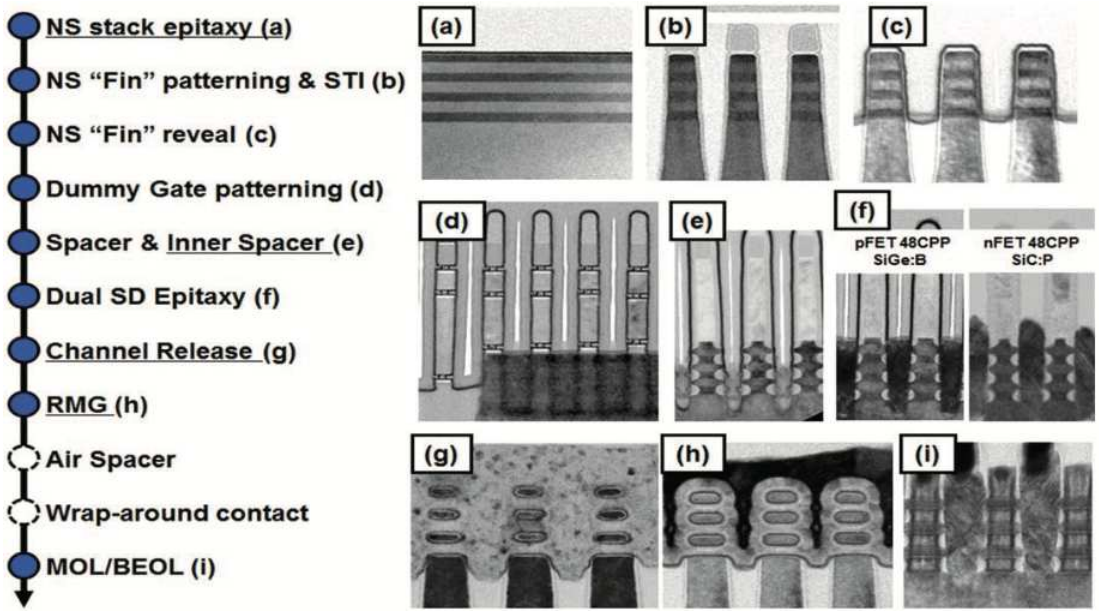

Figure II-5: Stacked nanosheet process sequence and TEM. IBM, Samsung Electronics, Global Foundries, (ref **[129]**).

Having established the hardware is so challenging, we know any system and component in custom or niche application will tend to degrade with time when operating under nominal or even sometimes extreme conditions. Yet the best reliable technology will continue to be affected by change in their intrinsic characteristic and performances or due to extrinsic high stress applied.

B. General overview in GaN device failure mechanisms

Normally-Off high power switching AlGaN/GaN-on-Si heterojunction transistors are promising for high reliability space application. Nevertheless, such and similar GaN technologies suffers well-known failure mode issues as studied since the last decade by several authors on gate current leakage increase or/and current collapse [42], [43], dynamic on-resistance with recovery effects [26], strain relaxations and trap charging effects [44], [45], TDDB mainly related to GaN MIS-HEMTS structures [46], PBTI of GaN MOSFETs [47]. From book chapter on Power GaN Devices M. Meneghini, G. Meneghesso and E. Zanoni [48] (Springer Ed. 2017) in chap. 13, J. Wuerfl (FBH, Berlin) describes the most relevant drift effects that limit the performance of GaN-based power transistors. Degradation and drift effects on semiconductor devices can affect their performances either reversibly or definitively. Many failure mechanisms have been identified and described showing they are imperative for predicting device performance in real system environment.

The effect of temperature on electronic devices is often assessed by extrapolating from accelerated tests at extremely high temperatures based on the Arrhenius law. This method is known to be not necessarily accurate for prediction, particularly when stress induced failures are driven by non-thermal dynamic electrical stresses. Theoretical work in kinetic theory, thermodynamics, and statistical mechanics have developed forms that contain exponential forms similar to Arrhenius. It is observed that the well-known Arrhenius law usually does apply, albeit with some modification, within existing models describing Physics of Failure. This is known, by example, in Black's law, Coffin-Manson or any application of Eyring's law. These include the effect of humidity or the hydrogen poisoning or other effects in semiconductors [5], [29], [21], [49], [50], [51], [52]. When these effects are simultaneously activated under multiple stress conditions inducing series of different failure modes and mechanisms, the standard reliability predictive models are questionable.

Hence regarding the Normally-Off eGaN-on-Si heterojunction transistors, a critical concern with such new technology is reliability. It is mandatory to study the role of temperature and biasing stress on the high-power degradation of this type of technology.

Quite a multitude of drift effects are influencing the performance of power switching devices, reduce switching efficiency and can compromise reliability. **Figure II-6: Schematic cross section of an AlGaN/GaN HEMT at different bias and trapping conditions (from ref).**extracted from ref [53] as well as Figure II-7 and Figure II-8 summarizes the most important reversible drift mechanisms observed in GaN transistors. Often the effects described above are correlated to each other resulting in a great variety of device parameter changes.

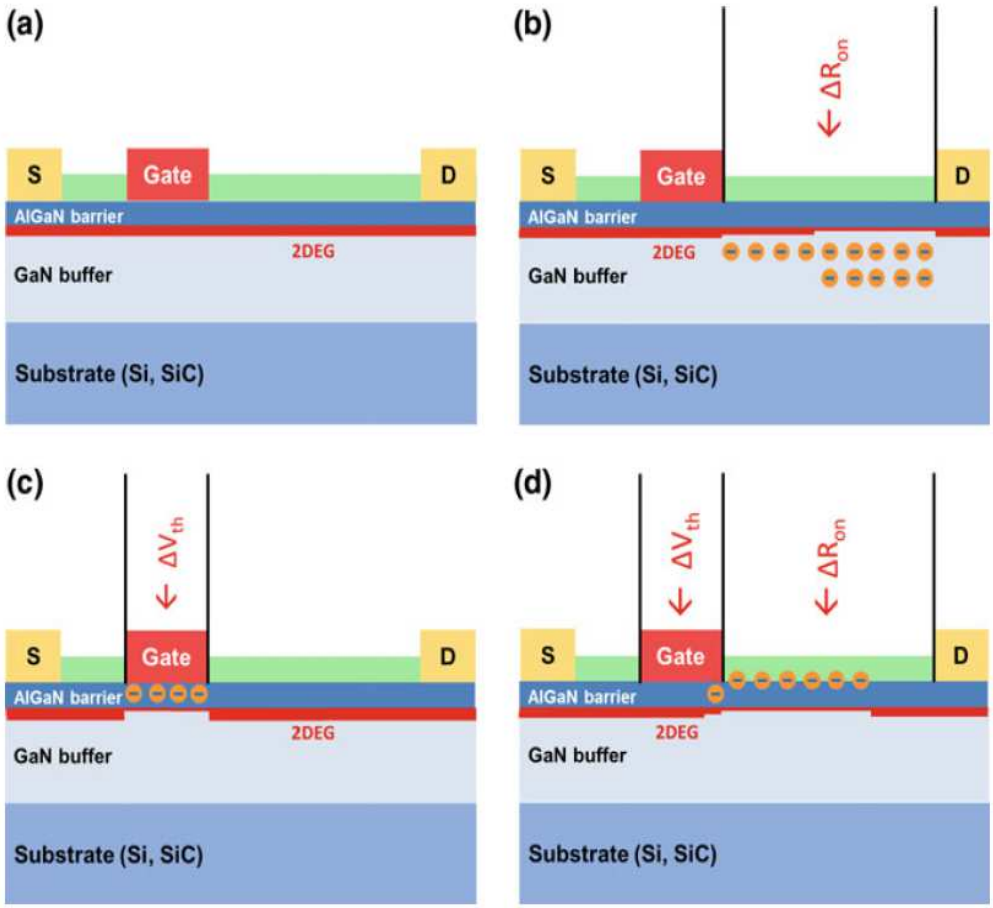

Figure II-6: Schematic cross section of an AlGaN/GaN HEMT at different bias and trapping conditions (from ref **[53]**).

a) Ideal device without any trapping at on-state: The 2DEG is fully populated with electrons.
b) Electron trapping in the vicinity of the drain access region: This situation, for example, happens immediately after switching from off-state to on-state at high drain bias. Trapped electrons (or depleted deep acceptors completely or partially deplete the 2DEG and hence impede current flow. If the source or the drain access regions are influenced by trapping, the on-state resistance changes. This gives rise to the so-called dynamic on-state resistance increase ΔR_{on_dyn}.
c) Electron trapping in the vicinity of the gate (underneath the gate) results in a partial depletion of the channel just underneath the gate: As these charges aid depleting the channel, a lower gate voltage is necessary to fully turn off the device—the threshold voltage shifts to more positive values.
d) Electron trapping at the interface to passivation layer and in the barrier layer: This leads to both a threshold voltage shift and to the formation of a virtual gate at the interface oriented towards the drain ⟶ reduction of 2DEG electron concentration, R_{on_dyn} increase.

Negative charges trapped in the source or drain access region, will reduce the 2DEG electron density resulting in an increase of on-state resistance. Traps confine to regions underneath the gate and in presence of negative charges the equilibrium must be compensated by a positive threshold voltage shift; collaterally threshold voltage can also shift in negative direction if positive charges are introduced (for example, if electrons are emitted from donor traps).

For GaN RF devices G. Meneghesso [54] degradation can still be observed on chosen parameters named "***indicators***" identified as key parameters showing pre-evolution of the future performance of a device.

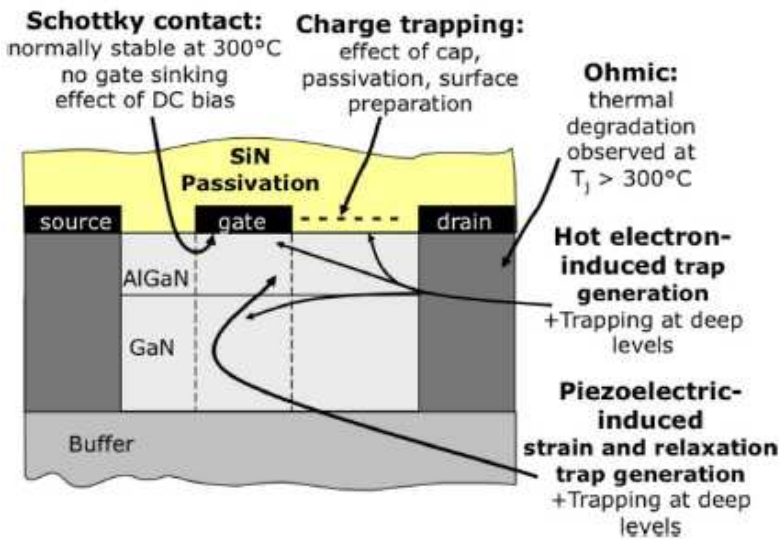

Figure II-7: Schematic cross section of an AlGaN/GaN HEMT RF transistor, identifying critical areas which can be subjected to degradation (as per ref. **[54]**)

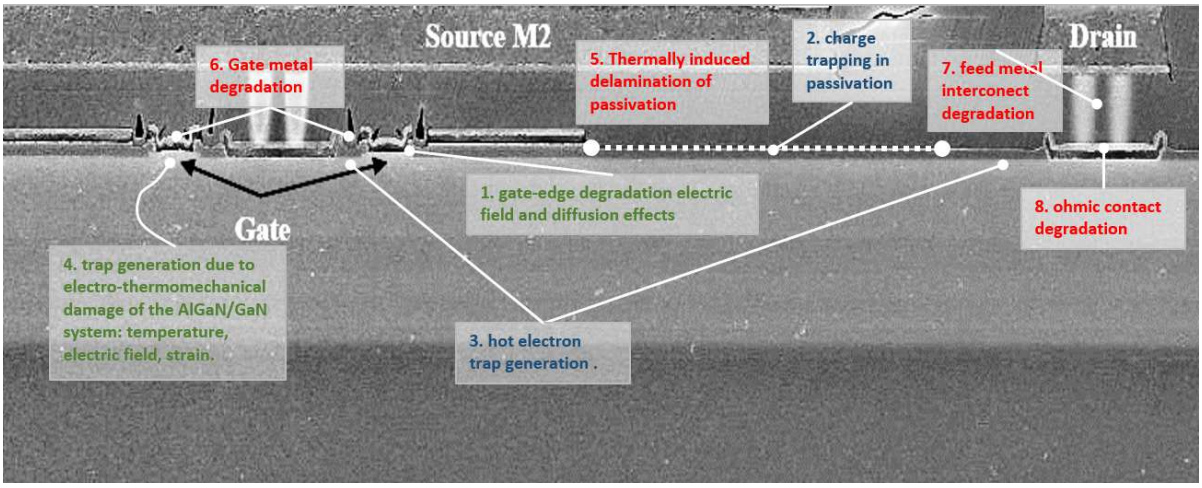

Figure II-8: Failure mechanisms recently identified on GaN HEMTs. Mechanisms identified in red (5, 6, 7, 8) are thermally activated mechanisms. Mechanisms 2 and 3 are related to the presence of hot electrons present at high bias conditions. Mechanisms 1 and 4 (green) are peculiar to GaN devices due to the polar and piezoelectric nature of this semiconductor. (freely arranged from ref. **[27]**)

C. Physical Reliability models applied to DSM technology

In a recent paper published in RAMS 2018 conference titled "Entropic Approach to Measure Damage with Applications to Fatigue Failure and Structural Reliability" [55], H. Yunm et al. suggest several entropies as candidates of proper damage measurements in fatigue process. The entropic approaches are expected to develop in order to apply them in practical reliability analyses and prognosis. The paradigm of the Transition State Theory (TST) developed by E. Wigner in 1934 [14] and by M. Evans, M. Polanyi in 1938 [13] is an approach we can benefit if we adapted to the concept of a unified semiconductor reliability model. Indeed in the early last century, the TST was applied to chemistry transformations by H. Eyring [21], and S. Glasstone et al. [15] in 1941. The TST was developed in chemistry based on the Hammond's postulate [16] published in 1955 applied to physical organic chemistry.

From the 60's and during the following 40 years, several authors report complementary reliability models centered around the mobile-ion (Na+) drift within dielectric [18], to intrinsic mechanism as TDDB [56] for example, while in mid-80's, J. W. McPherson and D.A. Baglee [22], [57] report of stress dependent activation energy and develop a generalized Eyring model in order to better understand thermally activated failure mechanisms (J.W. McPherson, Reliability Physics and Engineering – Time-to-Failure Modeling, 3rd ed., Springer, chapter 9 [23]).

Similarly in 2013, the stress dependent activation energy model based on Boltzmann-Arrhenius-Zhurkov model (BAZ) for

multiple stress proposed by E. Suhir [24], [25], [58] presented a generalization of the principle proposed by S.N. Zhurkov [59] in 1965 and also D.R. Cox [60], [20] in 1972. Suhir suggests to consider any type of stress (not only mechanical but also, electrical or external) as key parameters to modify the equivalent activation energy of a given failure mechanism. In other word, the activation cannot be considered as a constant parameter with respect to any type of stress (temperature range, biasing and signal stress range). We can view this approach as an equivalent TST concept applied to reliability paradigm [25].

Multiple failure mechanisms and Physics of degradation in semiconductors may occur in a single set of time-to-failure data but without obvious points of inflection to help separate the mechanisms. J. McPherson in his book 3rd edition of Reliability Physics and Engineering provides the basics of reliability modelling [23], [22] recalled *generally, materials/devices exist in metastable states. These states are referred to as being metastable because they are only apparently stable. Metastable states will change/degrade with time. The rate of degradation of the materials (and eventual time-to-failure for the device) can be accelerated by an elevated stress (e.g., mechanical stress, electrical stress, electrochemical stress, etc.) and/or elevated temperature*.

The Gibbs free energy description of material/device degradation is illustrated relating from ref [23] in Figure II-9, and Figure II-10. Considering the initial state to be a sound device before aging and the final state of a degraded device (either catastrophically failed or degraded and not compliant to the acceptable performance limit of the device). It is important to note at this point the reliability model is described by parameter drift degradation as a function of time and not as random failure paradigm. In this diagram the net reaction rate is a dynamic equilibrium between forward and reverse reaction meaning the degradation could be reversible. The net reaction process is written:

$$k_{Net} = k_{Forward} - k_{Reverse} \qquad \text{Eq. II-1}$$

With $k_{forward}$ and $k_{reverse}$ as function of temperature and stress S applied:

$$k_{Forward} = exp\left(-\frac{\Delta G_F^{\ddagger}(S,T)}{k \cdot T}\right) \qquad \text{Eq. II-2}$$

and

$$k_{Reverse} = exp\left(-\frac{\Delta H_R^{\ddagger}(S,T)}{k \cdot T}\right) \qquad \text{Eq. II-3}$$

Where T is the temperature in Kelvin, k the Boltzmann constant, and $\Delta G^{\ddagger}_{F}(S, T)$ represents the free energy of activation associated with the reaction process for the forward reaction. $\Delta H^{\circ}_{R}(S, T)$ represents the change in enthalpy required the final state reached for the reverse reaction. ΔS° is the entropy change, e.g. the driving force for a device degradation.

Figure II-9 represents the simplified Free Gibbs Energy diagram for a reaction activated only by the temperature for a sound device to a degraded device and vice-versa. Let's assume a device placed in an electronic system designed to implement an electronic function for a given application. The electronic function is supposed to fulfil a mission for a given life mission without failure, meaning without exceeding performance limits defined by the system functionality. In such condition a degraded device is defined as a device whose characteristics have changed to a certain extent above a given limit criteria fixed for the system to function properly. Let's call the final state to be the state the device is for the failure criteria to reach. So, the equations IV.1, 2 and 3 describe the probability the transition rates are associated to a "Sound device" to reach a failure limit.

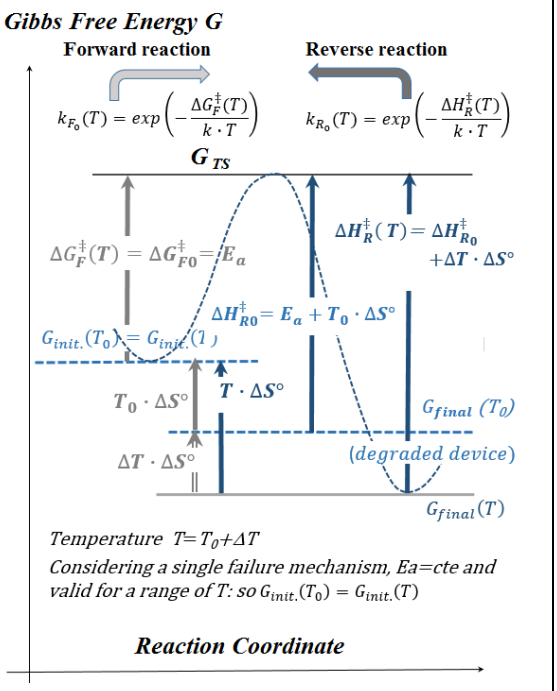

Figure II-9: Gibbs Free Energy diagram for *T* temperature increase applied, e.g. Arrhenius thermal activation energy diagram.

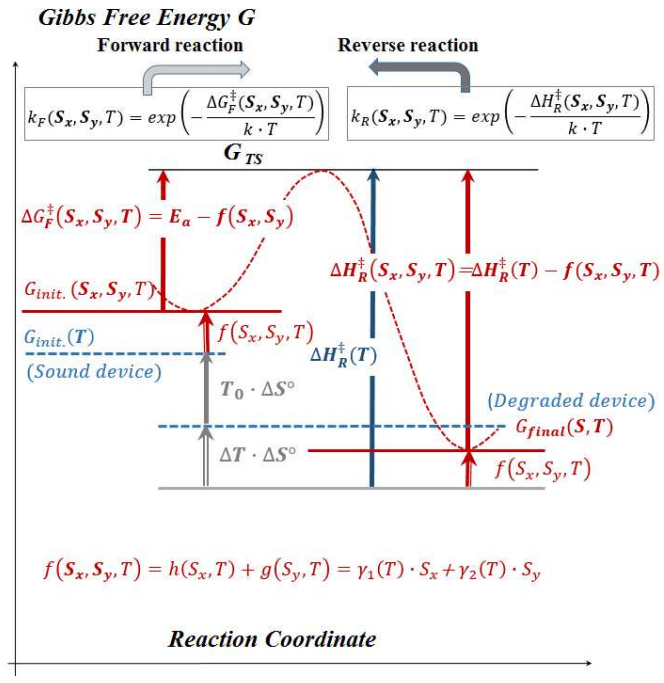

Figure II-10 : Gibbs Free Energy diagram considering reaction with two external stresses Sx and Sy applied and temperature T (diagram modified from ref **[23]**).

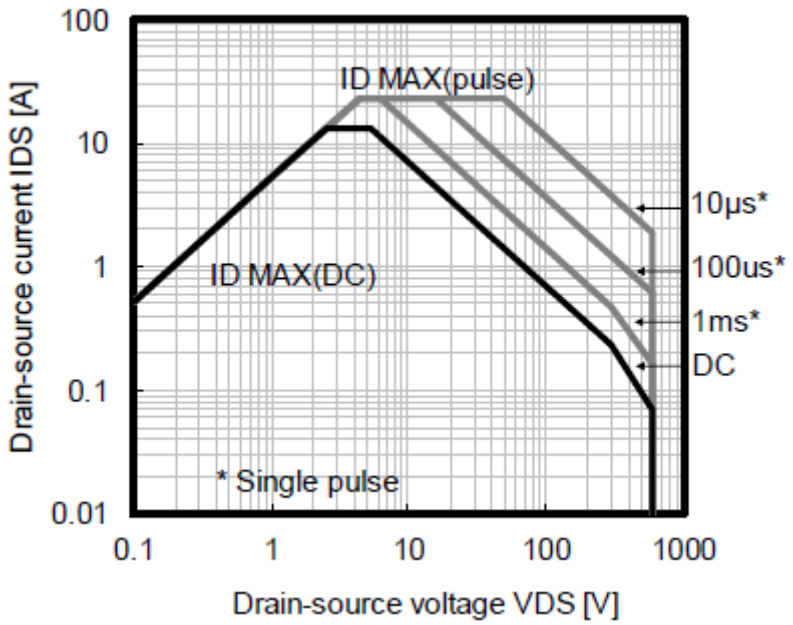

Figure IV.3: Example of Maximum rating and Safe Operating Area plot for a power transistor.

Figure II-10 is the Gibbs free energy diagram when considering multiple stress conditions and show how they impact the diagram. Note that the equivalent activation energy $\Delta G^{\ddagger}_{F}(S, T)$ is reduced when stresses are applied and can reduce to zero for extreme stress limit. So, a stress current may conduct to an instantaneous burnout catastrophic failure. As a consequence the energy barrier vanishes because of like a catalyst effect and the stress function $f(I_{burnout})$ compensate exactly the initial $\Delta G^{\ddagger}_{F0} = E_a$ at a given temperature T. So the equivalent activation energy range from E_a *(the Arrhenius pure thermal value)* to 0 for a current stress range for $0 \leq I \leq I_{burnout}$ or for $0 \leq I/Iburnout \leq 100\%$. Similarly, we can assume multiple stress to cumulate and the combination of them may reach the instantaneous catastrophic failure when the initial Arrhenius activation energy is fully compensated. These conditions can be compared when considering current, voltage and power dissipation parameters of a

transistor defined by their limits called Safe Operating Area as shown in the example given in figure 3. The static characteristics limits related to current (vertical axis), voltage (horizontal axis) and DC or pulsed power dissipation are plotted in log-log scale. In this case, the *I(V)* curves are limited by the power dissipation capability of the device (strait lines of the top right corner of the figure). The burnout can be reached either under high current or high voltage or high power overstresses. The combination of current and voltage stresses is seen through the power dissipation parameter: either one or the other or both lead to the destruction of the device. This paradigm can be modelled too by **Figure II-10**. It is worst to consider these parameters limits as static limits but similarly, dynamic and pulsed operation can be set.

From figure IV.2 we can observe the enthalpy $\Delta H_R^{\ddagger}(S=0,T_0)$ is by definition independent of the temperature variation ΔT because the transition state G_{TS} as well as the final state G_{final} is only related to initial T_0 value. We assume the expression of the enthalpy is:

$$\Delta \boldsymbol{H_R^{\ddagger}(S_i=0,T_0)=\Delta H_{R0}^{\ddagger}=E_a+T_0\cdot\Delta S^{\circ}} \qquad \text{for i = 1 , n} \qquad \text{Eq. II-4}$$

Let consider the case to superpose n stress conditions S_i. For the simplest case of n=2 stressors S_x and S_y,, a generalized Eyring model was established in ref [57] describing thermally activated failure mechanisms in materials/devices under stress as supported by figure IV.2. The forward reaction described by the Gibbs Free energy (respectively Enthalpy for the reverse reaction) is a function of the generalized stress *S*, and we set a Taylor Series expansion around point $(S_x, S_y)=(S_a, S_b)$ expanded to (limited to 1st order):

$$\boldsymbol{f(S_x,S_y,z)=f(S_a,S_b,c)+\frac{\partial f(S_a,S_b,c)}{\partial S_x}\cdot(S_x-S_a)+\frac{\partial f(S_a,S_b,c)}{\partial S_y}\cdot(S_y-S_b)} \qquad \text{Eq. II-5}$$

We consider the two infinitely differentiable functions $\Delta G^{\neq}_F (S_x, S_y, T)$ and $\Delta H^{\neq}_R (S_x, S_y, T)$ and limited to the Taylor series expansion linear around $(S_x, S_y) = (S_{a0}, S_{b0})$:

$$\Delta \boldsymbol{G_F^{\ddagger}(S_x,S_y,T)\approx\Delta G_F^{\ddagger}(S_{a0},S_{b0},T_0)+\left[\frac{\partial\left(\Delta G_F^{\ddagger}(S_x,S_y,T)\right)}{\partial S_x}\right]_{S_{a0},S_{b0}}\cdot(S_x-S_{a0})+\left[\frac{\partial\left(\Delta G_F^{\ddagger}(S_x,S_y,T)\right)}{\partial S_y}\right]_{S_{a0},S_{b0}}\cdot(S_y-S_{b0})} \qquad \text{Eq. II-6}$$

$$\Delta \boldsymbol{H_R^{\ddagger}(S_x,S_y,T)\approx\Delta H_R^{\ddagger}(S_{a0},S_{b0},T_0)+\left[\frac{\partial\left(\Delta H_R^{\ddagger}(S_x,S_y,T)\right)}{\partial S_x}\right]_{S_{a0},S_{b0}}\cdot(S_x-S_{a0})+\left[\frac{\partial\left(\Delta H_R^{\ddagger}(S_x,S_y,T)\right)}{\partial S_y}\right]_{S_{a0},S_{b0}}\cdot(S_y-S_{b0})} \qquad \text{Eq. II-7}$$

According to figure 1 and 2, we observe:

$$\Delta \boldsymbol{G_{F0}^{\ddagger}(T_0)=E_a} \quad \text{and} \quad \boldsymbol{E_a=\Delta H_{R0}^{\ddagger}-T_0\cdot\Delta S^{\circ}} \qquad \text{Eq. II-8}$$

$$\Delta \boldsymbol{H_R^{\ddagger}(S_x,S_y,T)=E_a+T\cdot\Delta S^{\circ}-\frac{1}{2}\cdot f(S_x,S_y,T)} \qquad \text{Eq. II-9}$$

$$\Delta \boldsymbol{G_F^{\ddagger}(S_x,S_y,T)=E_a-\frac{1}{2}\cdot f(S_x,S_y,T)} \qquad \text{Eq. II-10}$$

Let's assume simply $$\boldsymbol{f(S_x,S_y,T)=h(S_x,T)+g(S_y,T)} \qquad \text{Eq. II-11}$$

The factor ½ is set because we consider the same stress level affecting the entropy on the initial state of fig. 1.b and the enthalpy affecting the final state.

At zero stress the activation energy is converging to the standard Arrhenius thermal activation energy so we must assume (see fig. IV.2) $f(S_x=0, S_y=0) = 0$ and then

$$\boldsymbol{h(S_x = 0, T) = 0} \quad \text{and} \quad \boldsymbol{g\left(S_y = 0, T\right) = 0} \qquad \text{Eq. II-12}$$

According to Eyring law the stress function $f(S_x, S_y)$ is defined by :

$$\boldsymbol{h(S_x, T) = \gamma_1(T) \cdot S_x} \qquad \text{Eq. II-13}$$

and

$$\boldsymbol{g\left(S_y, T\right) = \gamma_2(T) \cdot S_y} \qquad \text{Eq. II-14}$$

We assume parameters $\gamma_1(T)$ and $\gamma_1(T)$ are defined by a temperature-dependence law of the form (see [57]:

$$\boldsymbol{\gamma_1(T) = a_0 + a_1 \cdot k \cdot T} \qquad \text{Eq. II-15}$$

$$\boldsymbol{\gamma_2(T) = b_0 + b_1 \cdot k \cdot T} \qquad \text{Eq. II-16}$$

Hence III.7.d, 8 and 9 combined give $f(S_{a0}, S_{b0}, T) = (a_0 + a_1 \cdot k \cdot T) \cdot S_{a0} + (b_0 + b_1 \cdot k \cdot T) \cdot S_{b0}$ Eq. II-17

From equations IV.7.c we get

$$\left[\frac{\partial\left(\Delta G_F^{\ddagger}(S_x,S_y,T)\right)}{\partial S_x}\right]_{S_{a0},S_{b0}} = \left[-\frac{\partial\left(f(S_x,S_y)\right)}{\partial S_x}\right]_{S_{a0},S_{b0}} = -\frac{1}{2}\cdot(a_0 + a_1 \cdot k \cdot T) \qquad \text{Eq. II-18}$$

and

$$\left[\frac{\partial\left(\Delta G_F^{\ddagger}(S_x,S_y,T)\right)}{\partial S_y}\right]_{S_{a0},S_{b0}} = \left[-\frac{\partial\left(f(S_x,S_y)\right)}{\partial S_y}\right]_{S_{a0},S_{b0}} = -\frac{1}{2}\cdot(b_0 + b_1 \cdot k \cdot T) \qquad \text{Eq. II-19}$$

The partial derivative of IV.7.b with respect to S_x *or* S_y gives

$$\left[\frac{\partial\left(\Delta H_R^{\ddagger}(S_x,S_y,T)\right)}{\partial S_x}\right]_{S_{a0},S_{b0}} = -\left[\frac{\partial\left(f(S_x,S_y)\right)}{\partial S_x}\right]_{S_{a0},S_{b0}} = -\frac{1}{2}\cdot(a_0 + a_1 \cdot k \cdot T) \qquad \text{Eq. II-20}$$

And

$$\left[\frac{\partial\left(\Delta H_R^{\ddagger}(S_x,S_y,T)\right)}{\partial S_y}\right]_{S_{a0},S_{b0}} = -\left[\frac{\partial\left(f(S_x,S_y)\right)}{\partial S_y}\right]_{S_{a0},S_{b0}} = -\frac{1}{2}\cdot(b_0 + b_1 \cdot k \cdot T) \qquad \text{Eq. II-21}$$

The parameters a_0, a_1, b_0, b_1 and $\Delta S°$ must be determined experimentally.
Consequently injecting equations IV.7, 10 and 11 into equations 6.a and 6.b, we obtain:

$$\Delta G_F^{\ddagger}(S_x,S_y,T) \approx E_a - \frac{1}{2}\cdot(a_0 + a_1 \cdot k \cdot T)\cdot S_{a0} - \frac{1}{2}\cdot(b_0 + b_1 \cdot k \cdot T)\cdot S_{b0} - \frac{1}{2}\cdot(a_0 + a_1 \cdot k \cdot T)\cdot(S_x - S_{a0}) - \frac{1}{2}\cdot (b_0 + b_1 \cdot k \cdot T)\cdot(S_y - S_{b0}) \qquad \text{Eq. II-22}$$

$$\Delta H_R^{\ddagger}(S_x,S_y,T) \approx E_a + T\cdot\Delta S° - \frac{1}{2}\cdot(a_0 + a_1 \cdot k \cdot T)\cdot S_{a0} - \frac{1}{2}\cdot(b_0 + b_1 \cdot k \cdot T)\cdot S_{b0} - \frac{1}{2}\cdot(a_0 + a_1 \cdot k \cdot T)\cdot(S_x - S_{a0}) - \frac{1}{2}\cdot (b_0 + b_1 \cdot k \cdot T)\cdot\left(S_y - S_{b0}\right) \qquad \text{Eq. II-23}$$

Which reduce to:

$$\Delta G_F^{\ddagger}(S_x,S_y,T) \approx E_a - \frac{1}{2}\cdot(a_0 + a_1 \cdot k \cdot T)\cdot S_x - \frac{1}{2}\cdot(b_0 + b_1 \cdot k \cdot T)\cdot S_y \qquad \text{Eq. II-24}$$

$$\Delta H_R^{\ddagger}(S_x,S_y,T) \approx E_a + T\cdot\Delta S° - \frac{1}{2}\cdot(a_0 + a_1 \cdot k \cdot T)\cdot(S_x) - \frac{1}{2}\cdot(b_0 + b_1 \cdot k \cdot T)\cdot\left(S_y\right) \qquad \text{Eq. II-25}$$

Let's define $S_x = x \cdot S_{Br1}$ and $S_y = y \cdot S_{Br2}$ Eq. II-26

and $S_{a0} = x_0 \cdot S_{Br1}$ and $S_{b0} = y_0 \cdot S_{Br2}$ Eq. II-27

where S_{Br1} and S_{Br2} are respectively the breakdown or burnout experimental values of the two stress parameters considered for S_x and S_y. In such a case the stress is defined by the percentages x and y respectively for S_x and S_y with $0 \leq x \leq 100\%$ and $0 \leq y \leq 100\%$.

$$\Delta G^{\ddagger}_{F_{LS}}(S_x, S_y, T) \approx E_a - \frac{1}{2} \cdot (a_0 + a_1 \cdot k \cdot T) \cdot x \cdot S_{Br1} - \frac{1}{2} \cdot (b_0 + b_1 \cdot k \cdot T) \cdot y \cdot S_{Br2} \quad \text{Eq. II-28}$$

$$\Delta H^{\ddagger}_{R_{LS}}(S_x, S_y, T) \approx E_a + T \cdot \Delta S^{\circ} - \frac{1}{2} \cdot (a_0 + a_1 \cdot k \cdot T) \cdot x \cdot S_{Br1} - \frac{1}{2} \cdot (b_0 + b_1 \cdot k \cdot T) \cdot y \cdot S_{Br2} \quad \text{Eq. II-29}$$

The net reaction rate under stress conditions for the breakdown process from equation IV.1 become:

$$k_{net_{LS}} = exp\left(-\frac{E_a - \frac{1}{2}(a_0 + a_1 \cdot k \cdot T) \cdot x \cdot S_{Br1} - \frac{1}{2}(b_0 + b_1 \cdot k \cdot T) \cdot y \cdot S_{Br2}}{k \cdot T}\right) - exp\left(-\frac{E_a + T \cdot \Delta S^{\circ} - \frac{1}{2}(a_0 + a_1 \cdot k \cdot T) \cdot x \cdot S_{Br1} - \frac{1}{2}(b_0 + b_1 \cdot k \cdot T) \cdot y \cdot S_{Br2}}{k \cdot T}\right) \quad \text{Eq. II-30}$$

Hence, equation III.16 expresses with a thermal term related to the activation energy as a function of stress conditions in a like-catalyst thermodynamic process and a stress term depending of the stresses applied in the form (same conclusion as ref [24]):

$$k_{net} = k_1(x, y) \cdot exp\left(-\frac{E_{a_{equ}}(x,y)}{k \cdot T}\right) \quad \text{Eq. II-31}$$

with $$\boldsymbol{E_{a_{equ}}(x, y) = E_a - \frac{1}{2} \cdot a_0 \cdot x \cdot S_{Br1} - \frac{1}{2} \cdot b_0 \cdot y \cdot S_{Br2}} \quad \text{Eq. II-32}$$

and $k_1(x, y) = k_0 \cdot exp\left(\frac{1}{2} \cdot a_1 \cdot x \cdot S_{Br1} + 1/2 \cdot b_1 \cdot y \cdot S_{Br2}\right)$ and $k_0 = \left(1 - exp\left(-\frac{\Delta S^{\circ}}{k}\right)\right)$ Eq. II-33

From these equations we can observe the **equivalent activation energy is dependent of the temperature T_0 and is increasing with temperature**. So, under the stress conditions, **the failure mechanism model is a non-uniform acceleration mechanism**.

We can also observe the equivalent activation energies is based on the **constant Arrhenius activation energy** E_a of the mechanism under investigation but modified by a series of factors related to the stress condition applied.

Accelerating factor can be expressed considering range stress conditions. We can simply write the *AF* considering operational conditions versus reference stress conditions (sub-labelled 'op' respectively 'ref') as follows:

$$AF(x_{op}, y_{op}, T_{op}, x_{ref}, y_{ref}, T_{ref}) = exp\left[-\frac{E_a}{k}\left(\frac{1}{T_{op}} - \frac{1}{T_{ref}}\right)\right] \cdot exp\left[\frac{a_0 \cdot S_{Br1}}{2 \cdot k}\left(\frac{x_{op}}{T_{op}} - \frac{x_{ref}}{T_{ref}}\right)\right] \cdot exp\left[\frac{b_0 \cdot S_{Br2}}{2 \cdot k}\left(\frac{y_{op}}{T_{op}} - \frac{y_{ref}}{T_{ref}}\right)\right] \cdot exp\left[\frac{a_1}{2} \cdot S_{Br1} \cdot (x_{op} - x_{ref}) + \frac{b_1}{2} \cdot S_{Br2} \cdot (y_{op} - y_{ref})\right] \quad \text{Eq. II-34}$$

Precautions associated with accelerated testing

The x and y values are assumed to range from no stress (e.g. x=y=0%) to highest stress (e.g. x=y=100%) and the AF expression is exact for any range of external stress applied. These theoretical calculations must be taken with extreme cautions. As we use to set the acceleration is supposed to be related to failure physics without changing the physics. Indeed, assuming a single failure mechanism of PoF, the accelerating factor calculated for various stress conditions superimposed, is non-uniform and the equivalent activation energy is stress and temperature dependent. This must be verified using Weibull (or lognormal) distributions when conducting proper test experiments and observing a single value of E_a activation energy parameter determined within a limited domain of range of temperature.

Based on failure rate expression the time-to-failure for reference stress accelerated conditions (REF) compared to operational condition (labelled 'op') becomes:

$$TTF_{50\%}\left(S_{x_{op}}, S_{y_{op}}, T_{op}\right) = TTF_{50\%}(S_{REF}, S_{REF}, T_{REF}) \cdot exp\left[\frac{E_a}{k}\left(\frac{1}{T_{REF}} - \frac{1}{T_{op}}\right)\right] \cdot exp\left[\frac{a_0 \cdot S_{Br1}}{2 \cdot k}\left(\frac{x_{op}}{T_{op}} - \frac{x_{REF}}{T_{REF}}\right)\right] \cdot exp\left[\frac{b_0 \cdot S_{Br2}}{2 \cdot k}\left(\frac{y_{op}}{T_{op}} - \frac{y_{REF}}{T_{REF}}\right)\right] \cdot exp\left[\frac{a_1}{2} \cdot S_{Br1} \cdot (x_{op} - x_{REF}) + \frac{b_1}{2} \cdot S_{Br2} \cdot \left(y_{op} - y_{REF}\right)\right] \quad \text{Eq. II-35}$$

These mathematics and physic approaches show how the activation energy is related to the stress and temperature applied

and can no-longer be considered as a constant to extrapolate some experiment under high stress to nominal mission operation profile. That's the reason why several end-user Industries and Institutions are very cautious to perform lifetest conditions as close as the nominal conditions because of the change of activation energy attributed sometime wrongly to new (or different) failure mechanism while it is simply explained by the interaction of stress and temperature effect on the measured activation energy or to a best extend to Eyring law.

One may note the burnout limits S_{Br1} and S_{Br2} are characteristic parameters which may change during aging. These limits can drift also during aging time and hence as the stress applied S_x or S_y (eq. III.14) this means the x and y percentage stress values increase during aging from low stress level to high stress level.

The general statement that during useful life the failure rate is supposed to be constant can be wrong when approaching the end of life. When devices get closer to the wearout occurrence, it is assumed they degrade faster and their burnout limit reduces when time elapse. In such a way, the applied stress cannot be considered constant and is reaching high-stress level comparatively to initial low stress.

This observation can give some insight to describe how the failure rate can be considered as non-constant and hence to propose a vision on EOL of the bathtub curve.

D. Reliability and probability mathemathics

Reliability is defined as the probability that a device will function over some period of time, and usually is measured in Failures-In-Time units (FIT units). The FIT is a rate, defined as the number of expected device failures per 10^9 parts-hours.

Failure Rate (λ) is calculated by dividing the total number of failures or rejects by the cumulative time of operation. In the HTOL model, the cumulative time of operation is referred to as Number of Device Hours (NDH):

$$NDH = D \cdot H \cdot A_F \qquad \text{Eq. IV-36}$$

where: D = Number of Devices Tested
H = Test Hours per Device
A_F = Acceleration Factor derived from the Arrhenius equation and or other stressor.

A FIT is assigned to each component multiplied by the number of devices in a system as an approximation of the expected system reliability. For the reliability model of an entire system, the FIT rates of each component in the system are summed together.

The *Failure Rate (λ)* in FITs (Failures per billion unit-hours) is given by:

$$\lambda = \frac{\#\cdot failures}{NDH} \qquad \text{Eq. IV-37}$$

The conventional chi-squared expression for failure rate, λ, is:

$$\lambda = \frac{\chi^2(2n+2,1-\alpha)\cdot 10^9}{2\cdot D\cdot H\cdot A_F} \qquad \text{Eq. IV-38}$$

Where $\frac{\chi^2(2n+2,1-\alpha)}{2}$ is the upper confidence value for "n" failures and upper confidence limit, α (expressed in %). The value for 2n + 2 degrees of freedom and the probability, 1 – α, can be obtained from a table or calculated using Microsoft Excel functions.

According to this expression, to demonstrate zero failure rate must account either a sample size to go to infinity, AF to go to infinity or test time to go to infinity [61]. In such case we get no product to ship the accelerating factor cannot be infinity because physically impossible) or test time will end when products are too old to ship. Achieving a zero-failure rate goal using reliability testing is impossible.

A practical numerical application from Standard Device Qualification from HTOL qualification sequence leads to the following limitation:

For defect density limits:

let's assume 0 failures on 92 devices sample size (SS) under tests, a 60% confidence level applied on a Poisson distribution is expressed as:

$$F \leq \frac{1}{SS}\cdot ln\left(\frac{1}{1-P}\right) = \frac{1}{92}\cdot ln\left(\frac{1}{1-0.6}\right) = 0.025 = 2{,}5\% \text{ or } 25\,000 \text{ ppm.} \qquad \text{Eq. IV-39}$$

Numerical application for a study case on a FinFET technology assuming 3 major failure mechanisms defined by the following Arrhenius reliability parameters (not considering other type of stressors like voltage or current for sake of simplification):

- EM- Electromigration kinetics (Ea=0.75eV (Al-Cu),

- NBTI kinetics (Ea=0.6eV),
- HCI kinetics (Ea=-0.25eV long channel or +0.25 short channel).

Assuming a qualification test experiment on 130 samples tested during 2000 hrs of 150°C HTOL with 0 failure observed.

What would be the device operating projected lifetime verified if the operational application is at T=45°C ?
In such case, what are the failure rates λ_i (for i=EM, NBTI or HCI) in FIT and the corresponding accelerating factors for each mechanism?
What are the Time-To-Failure for each failure mechanism considering a constant failure rate based on a Poisson statistic?
What would be the equivalent total λ_{total} and corresponding Time-To-Failure if all failure mechanisms are equally activated?

The hypotheses are summarized in table IV-1.a and some answers are shown to the questions above in Table IV-1.b.

Qualification test conditions		
Sample Size	130	
duration	2000	hrs
nb of hr.comp.	260000	hr.comp.
Tstress for high temp. (EM, BTI and HCI short channel)	150	°C
Tstress for HCI long channel	0	°C
Tuse	45	°C
k (Boltzmann factor)	8,62E-05	eV/°K
CL	90%	

Table IV-1.a: Example of qualification test condition for a CMOS FinFET technology with an example of associated list of failure mechanisms.

Reliability figures			Failure mechanisms	AF	Operational time verified (in years)	λ Poisson (in FIT) in operation	MTBF (in years) $1/\lambda$ Poisson	CDF *Fpoisson* (@ t = 30 ans)
Ea EM	0,75	eV	Ea EM Tref= 150°C	892	204	10	11501	0,26%
Ea NBTI	0,6	eV	Ea NBTI Tref= 150°C	229	52	39	2955	1,01%
Ea HCI	0,25	eV (short channel)	Ea HCI (short channel) Tref= 150°C	9,6	2,2	920	124	21,48%
Ea HCI	-0,25	eV (long channel)	Ea HCI (long channel) Tref=0°C	4,5	1,03	1969	58	40,39%
						λ total	MTBF equ.	CDF *Fpoisson* (@ t = 30 ans)
						2937	39	53,78%

Table IV-1.b: CMOS FinFET technology reliability assessment to predict operational time duration and CDF, MTTF for various failure mechanisms for CL=90%.

From table IV-1.a we consider a lot of 130 sample used to validate a qualification test sequence as defined by Quality Standards with two kind of lifetest conditions: one at high temperature (150°C) to stress EM, BTI and HCI for short channel transistors and one a low temperature (0°C) stress applicable to long channel based transistors (HCI mechanism has a negative activation energy).

According to the lifetest sequence duration, the number of hours.components is 260,000.

What should be the sample size and duration to demonstrate a cumulative CDF equal of less than 0.1% after 30 years (as needed in Space application)? Considering all failure mechanisms activated simultaneously (according to table IV-1.a), the answer is summarized in table IV-A.c and it is required to test a 200 Mhrs.comp (or 200,000 parts tested for 1,000 hrs) to guarantee the 0.1% CDF goal after 30 years at 90%CL. In such a case the failure rate λ_{total} is 3.8 FIT, MTBF is about 29.9 Kyears and the $F_{poisson}$ (CDF) after 30 years is as low as the 0.1% goal.

To demonstrate 30 years for CDF less than 0.1%	20000	Sample size	2E+08 hr.comp	λ_{total}	MTBF equ. (in years)	CDF *Fpoisson* (@ t = 30 years)
	10000	hrs		3,82	29898	0,10%

Table IV-1.b: CMOS FinFET technology. What should be the sample size and duration to demonstrate a cumulative CDF equal of less than 0.1% after 30 years with 90%CL.

The accelerating factors at 90% confidence level range broadly from 892 down to 4.5. The device operating projected lifetime (CL 90%) verified by the qualification stress test is projected for the operational application duration at T=45°C up to 204 years for EM mechanism, 52 years for NBTI, 2.2 years for Hot HCI and 1 year for Cold HCI mechanisms. This shows how much multiple failure mechanisms can affect the demonstrated operating time projection.

Respectively, the failure rate projected in operation assuming a Poisson distribution at 90% CL is assessed 10 FIT for EM, 39 FIT for NBTI, 920 FIT for hot HCI, and 1,969 FIT for Cold HCI. These results are not enough to prove application reliability goals.

If supposed disjointed, each failure mechanism leads to a wide range of TTF from 1,1501 years for EM, 2,955 years for NBTI, 124 years for Hot HCI and 58 years for Cold HCI. Again these figures must be considered from a different point of view to be representative of the theoretical truth.

Because of this large variety of values, we need to suppose all failure mechanisms EM, BTI and hot HCI are equally and simultaneously activated. So, we need to cumulate their corresponding $\lambda_{Poisson}$ distribution to assess a total equivalent failure rate. This sum gives λ_{total} (CL90%)= 2,937 FIT for Poisson distribution at 90%CL. Then the total MTTF is about 39 years for a Poisson distribution and not as supposed if we take into account the worst case of each failure mechanism.

We have to be careful considering these results because they are first extracted from a single lot testing and a reduced number of device. The statistic helps to predict how long a device from such a tested long sequence can be operational without any failure (still with 90% confidence level). The true λ and TTF are expected to be much greater than the values calculated. The occurrence of various failure mechanism must be considered with some caution as their activation is strongly dependent of the conditions of test which can be far from the operational one's.

A last comment is that these failures are supposed to be constant with time (the bottom of the bathtub curve) but this is wrong way to address end of life reliability figure. We know that the failure mechanisms must be considered as wearout (to the end of the bathtub curve) and we should take into consideration WEIBULL (or LOGNORMAL respectively) distribution to determine the $MTTF_{wearout}$ as 63% lot failure (respectively 50% lot failure). This causes that the $MTTF_{wearout}$ is not the MTTF deduced from the constant failure rate.

Therefore, Standard HTOL is relatively poor to predict MTTF associated constant failure rate and ineffective for wearout modelling as no failure are observed. Furthermore, the MTTF is not a zero-failure guarantee (is a 50% lot failure) and we should define rather a $MTTF_{0.1\%}$ for high reliability application.

Continuing we can question, how many devices would you need to test to assure that the fraction defective is F$\leq$ 35 ppm?

Answering such a question need to invoke the "Stress-Resistance" concept. The implementation of the "Stress-Resistance" method usually refers to information called "lump sum". The most basic version of the "Stress-Resistance" method calculates the probability of failure which results from the interaction between two probability laws. In general, if any two laws are explicitly known, the probability of failure can be calculated by numerical resolution of a convolution integral. Only a few particular cases lead to purely analytical solutions, when the two laws belong to the same statistical family. Among the most classic examples, we can cite the interaction between pairs of counterpart laws, normal or log-normal, which allow to obtain exact analytical solutions as presented by L. Pierrat [62], and D. Delaux. [63]. Nevertheless, assuming correct hypotheses, approximation can be set [64]. At the 60% confidence level (P=0.6) and with accepting on finding zero defects (x=0) the sample size (SS) is deduced from various statistical distributions:

$$\text{Poisson: } SS = \frac{1}{F} \cdot ln\left(\frac{1}{1-P}\right) = \frac{1}{35ppm} \cdot ln\left(\frac{1}{1-0.6}\right) = 26{,}180\ devcies$$

$$\text{Chi Square: : } SS = \frac{[\chi^2(P,2)]/2}{F} = \frac{[\chi^2(0.6,2)]/2}{35\ ppm} = \frac{1.8326/2}{35\ ppm} = 26{,}180\ devices$$

So above sample size SS>50, little or no differences is observed in statistical distributions. In fact, such situations are not

entirely realistic, because in general, the laws resulting from statistical estimates deviate from the theoretical laws to which they are assimilated.

The acceleration factor, AF, is the most problematic consideration. The industry recognizes that an AF is given only for each failure mechanism individually by specific testing from the manufacturer, and is defined as the ratio between the time it takes a certain fraction of the devices to fail, under a certain amount of stress or use conditions, and the corresponding time under more severe stress or use conditions. In the case of multiple mechanisms, the TTF for each mechanism must be considered separately for each associated AF per mechanism.

The Time-to-Failure (TF) of each mechanism can also be defined from the physical models of the mechanisms, which are described on the JEDEC publication JED-122G [5] (see also ref [23]):

TDDB anode hole injection exponential 1/E model (Chen & Hu 1985) from Fowler-Nordheim tunnelling current:

$$TF_{TDDB_{\frac{1}{E}model}} = e^{G(T)\cdot\frac{1}{E_{0x}}} \cdot e^{\frac{Ea_{TDDB}}{k\cdot T}} \quad \text{Eq. IV-36}$$

TDDB thermoelectrical exponential E model (McPherson & Baglee 1985)

$$TF_{TDDB_{Emodel}} = e^{\gamma(T)\cdot E_{ox}} \cdot e^{\frac{Ea_{TDDB}}{k\cdot T}} \quad \text{Eq. IV-40}$$

TDDB Power Law voltage V-model for hyper-thin Si02 dielectrics (<40Å)

$$TF_{TDDB_{Power\ lawmodel}} = B_0(T) \cdot {V_{ox}}^{-n} \cdot e^{\frac{Ea_{TDDB}}{k\cdot T}} \quad \text{Eq. IV-41}$$

TDDB exponential $E^{1/2}$ model

$$TF_{TDDB_{E1/2model}} = C_0(T) \cdot e^{-\alpha\cdot\sqrt{E}} \cdot e^{\frac{Ea_{TDDB}}{k\cdot T}} \quad \text{Eq. IV-42}$$

Hot Carrier Injection (Takeda 1983)

$$AT = f \cdot \left(\frac{I_{sub}}{W}\right)^{-N} \cdot e^{\frac{Ea_{HCI}}{k\cdot T}} \quad \text{Eq. IV-43}$$

Negative-Bias Temperature Instability

$$TF_{NBTI} = V^{\frac{\alpha}{m}} \cdot e^{\frac{Ea_{NBTI}}{k\cdot T}} \quad \text{Eq. II-44}$$

Electromigration (Black 1969)

$$TF_{EM} = A_0 \cdot (J - J_{crit})^{-p} \cdot e^{\frac{Ea_{EM}}{k\cdot T}} \quad \text{Eq. IV-45}$$

Stress migration (McPherson & Dunn 1987) due to mechanical stress inducing plastic deformation of metal with time

SM in Aluminium or Copper interconnects

$$Creep(voiding)rate = B_0 \cdot (T_O - T)^n \cdot e^{\frac{Ea_{SM_{Al}}}{k\cdot T}} \quad \text{Eq. IV-46}$$

Humidity model (HM) exponential reciprocal-humidity

$$TF_{HM_{exp-reciprocal}} = A_0 \cdot e^{\frac{b}{RH}} \cdot e^{\frac{Ea_{HM}}{k\cdot T}} \quad \text{Eq. IV-47}$$

Humidity model (HM) power law humidity model

$$TF_{HM_{power-law}} = A_0 \cdot RH^{-n} \cdot e^{\frac{Ea_{HM}}{k\cdot T}} \quad \text{Eq. IV-48}$$

Humidity model (HM) exponential humidity model

$$TF_{HM_{power-law}} = A_0 \cdot e^{-a\cdot RH} \cdot e^{\frac{Ea_{HM}}{k\cdot T}} \quad \text{Eq. IV-49}$$

Thermal-cycling/Fatigue induced mechanisms

Coffin-Manson model for low-cycle fatigue

$$\#Cycle - to - Failure = A_0 \cdot \left(\Delta\varepsilon_p\right)^{-s} \quad \text{Eq. IV-50}$$

Where $\Delta\varepsilon_p$ is the plastic strain range.

Coffin-Manson model for temperature cycling

$$\Delta\varepsilon_p \propto (\Delta\mathrm{T} - \Delta\mathrm{T}_0)^{\beta} \quad \text{Eq. IV-51}$$

Failure rates are often expressed in term of failure units (FITs): 1*FIT* = 1 failure in 10^9 device-hours.

TTF is statistical and a distribution of time-to-failure is observed. Life distributions are defined based on three mathematical functions:

a) the probability density function for device or system failures *f(t)* which relate the relative frequency of failure to time, *t* ;
b) the cumulative distribution function, *F(t)*, which gives the summation of failure proportion to that time.
c) The curve of failure rate *λ(t)*

The instantaneous failure rate, the hazard rate function *λ(t)*, is the ratio of the number of failures during the time period Δt, for the devices that were healthy at the beginning of testing (operation) to the time period Δt.

$$\lambda(t) = \frac{f(t)}{1-F(t)} \quad \text{Eq. IV-52}$$

The cumulative probability distribution function (CDF) *F(t)* for the probability of failure is related to the probability density distribution function *f(t)* as

$$F(t) = \int_0^t f(x) \cdot dx \quad \text{Eq. IV-53}$$

and the reliability function *R(t)*, the probability of non-failure is defined as

$$R(t) = 1 - F(t) \quad \text{Eq. IV-54}$$

Probability data obtained when performing accelerated tests can be modeled by various distribution models, such as exponential law, Weibull law, normal or log-normal distributions, beta distributions, etc. The main life distribution functions are:

- Exponential
- Normal
- Lognormal
- Weibull distribution

Exponential distribution summary:

Probability density function $f(t) = \lambda \cdot e^{-\lambda \cdot t}$ Eq. IV-55

Cumulative density function: $F(t) = 1 - e^{-\lambda \cdot t}$ Eq. IV-56

Instantaneous Failure Rate, hazard rate: $\lambda(t) = \lambda$ Eq. IV-57

Significant properties

Mean (average) of MTBF: $MTBF = \frac{1}{\lambda}$

Normal distribution summary:

Probability density function $f(t) = \frac{1}{\sigma \cdot \sqrt{2\pi}} \cdot e^{-\frac{1}{2}\cdot\left(\frac{t-\mu}{\sigma}\right)^2}$ Eq. IV-58

Cumulative density function: $F(t) = \frac{1}{\sigma \cdot \sqrt{2\pi}} \cdot \int_0^t e^{-\frac{1}{2}\cdot\left(\frac{x-\mu}{\sigma}\right)^2 \cdot dx}$ Eq. IV-59

Instantaneous Failure Rate, hazard rate: $\lambda(t) = \frac{\frac{1}{\sigma \cdot \sqrt{2\pi}} \cdot e^{-\frac{1}{2}\left(\frac{t-\mu}{\sigma}\right)^2}}{1-\frac{1}{\sigma \cdot \sqrt{2\pi}} \int_0^t e^{-\frac{1}{2}\left(\frac{x-\mu}{\sigma}\right)^2 \cdot dx}}$ Eq. IV-60

Significant Distribution properties

Median (50% failure): $t = t_{50\%} = \mu$
Mean (average): $t = \mu$
Location parameter: μ
Shape parameter: σ
s, estimate of σ can be calculated as $t_{50\%} - t_{16\%}$

Weibull distribution summary:

Probability density function $f(t) = \frac{\beta \cdot (t-\gamma)^{\beta-1}}{\alpha^{\beta}} \cdot e^{-\left(\frac{t-\gamma}{\sigma}\right)^{\beta}}$ Eq. IV-61

Cumulative density function: $F(t) = 1 - e^{-\left(\frac{t-\gamma}{\sigma}\right)^{\beta}}$ Eq. IV-62

Instantaneous Failure Rate, hazard rate: $\lambda(t) = \frac{\beta \cdot (t-\gamma)^{\beta-1}}{\alpha^{\beta}}$ Eq. IV-63

Significant properties
Location parameter (63% failure): $t_{63\%} = \alpha$
Shape parameter: β
Time-delay parameter = γ, a factor used only when the data do not fit the distribution, except with the use of a time delay.

Lognormal distribution summary:

Probability density function: $f(t) = \frac{1}{\sigma \cdot t \cdot \sqrt{2\pi}} \cdot e^{-\frac{1}{2} \cdot \left(\frac{\ln t - \mu}{\sigma}\right)^2}$ Eq. IV-64

Cumulative density function: $F(t) = \frac{1}{\sigma \cdot \sqrt{2\pi}} \cdot \int_0^t \frac{1}{x} \cdot e^{-\frac{1}{2} \cdot \left(\frac{\ln x - \mu}{\sigma}\right)^2} \cdot dx$ Eq. IV-65

Instantaneous Failure Rate, hazard rate: $\lambda(t) = \frac{\frac{1}{\sigma \cdot t \cdot \sqrt{2\pi}} \cdot e^{-\frac{1}{2}\left(\frac{\ln t - \mu}{\sigma}\right)^2}}{1 - \frac{1}{\sigma \cdot \sqrt{2\pi}} \cdot \int_0^{t} \frac{1}{x} \cdot e^{-\frac{1}{2}\left(\frac{\ln x - \mu}{\sigma}\right)^2} \cdot dx}$ Eq. IV-66

Significant properties
Median (50% failure): $t = t_{50\%} = e^{\mu}$
Mean (average): $t = e^{\mu + \frac{\sigma^2}{2}}$
Location parameter: e^{μ}
Shape parameter: σ
s, estimate of σ can be calculated as $\ln \frac{t_{50\%}}{t_{16\%}}$
Their schematic representation behaviors are given in Figure IV.4.

When considering devices or system life, three failure types can be distinguished and are commonly represented by the bathtub curve (see Fig. IV.7).

Failures that appear during the early period of component life and are called early (infantile) failures. They can be explained through a faulty manufacture and an insufficient quality control in the production. They can be eliminated by a systematic screening test. But some component weaknesses can pass through this filter for several reasons either because the screening stress test conditions are not high enough effective to screen the latent defects or because the failure criteria set is defined for eliminating catastrophic failures and some level of drift failures.

Random failures, the second category, can't be eliminated neither by a screening test, nor by an optimal use politics (maintenance). They can be provoked by sudden voltage increases that can strongly influence the component quality and reliability. These failures appear erratically, accidentally, unforeseeably. In paper written in 2019, by Ed Sperling, the editor in chief of Semiconductor Engineering [65], presented automakers' interviews and as said by Gert Jørgensen, vice president of marketing at Delta Microelectronics "You can't test for the random failures random failures and latent defects add their own challenges. Sperling argue "the problem is worse in automotive due to both the expected lifespan of systems and the harsh environmental conditions. True random failures are rare. A stray alpha particle hitting a circuit and causing damage is known to happen, and the chances of that occurring increase with denser circuits and thinner insulation. So a single-event upset affecting 7nm device with FinFETs packed tightly together is more likely than at 28nm. The same is true for random contaminants, which may affect one part differently than another. But delineating which failures are truly random from those that are not is time-consuming, and that adds to the cost and slows down time to market."

Wearout failures, the third category, constitute an indicator of the component ageing.

Two methods are generally used to make reliability estimates: (i) parts counts method and (ii) parts stress analysis method. The parts counts method requires less information, generally that dealing with the quantity of different part types, quality level of the parts, and the operational environment.

Parts stress analysis requires the greatest amount of details and is applicable during the later design phases where actual hardware and circuits are being designed.

Whichever method is used, the objective is to obtain a reliability estimate that is expressed as a failure rate. Calculation of failure rate for an electronic assembly, unit or system requires knowledge on the failure rate of each part contained in the item of interest. If we assume that the item will fail when any (all in series) of its parts fail, the failure rate of the item will equal the sum of the failure rate of its parts.

Parts count reliability prediction [4], [66]: the information needed to use the method is: (i) generic part types (including complexity of microelectronics) and quantities; (ii) part quality levels; and (iii) equipment environment. The general expression for equipment failure rate with this method is for given environmental conditions:

$$\lambda = \sum_{i=1}^{n} N_i \cdot \left(\lambda_G \cdot \pi_Q\right)_i \qquad \text{Eq. IV-67}$$

Where :

λ = total equipment failure rate (in FIT = 1 failure in 10^9 hrs)
λ_G = generic failure rate for the i^{th} generic part
π_Q = quality factor for the i^{th} generic part
N_i = quantity of i^{th} generic part
n = number of different generic parts.

In Parts stress analysis method, part failure models vary with different part types, but their general form is:

$$\lambda_i = \lambda_B \cdot \pi_E \cdot \pi_A \cdot \pi_Q \ldots \pi_N \qquad \text{Eq. IV-68}$$

Where:

λ_B = reference failure rate without environmental stress

π_E = environmental factor for accounting for other than temperature stressors (e.g. external stressors like vibration, humidity, etc

π_A = adjustment factors as for example biasing conditions (either static or dynamic or signal stressors, etc)

π_Q = quality factor referring to the quality control applied during manufacturing, screening, lot assurance testing before shipment to user.

Life distributions	Probability density function *f(t)*	Reliability function *R(t)*	Hazard Failure Rate $\lambda(t)$
Normal	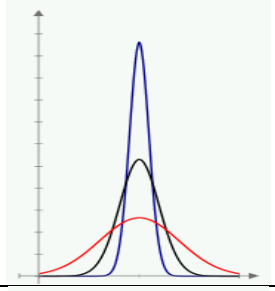	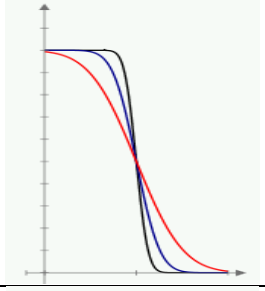	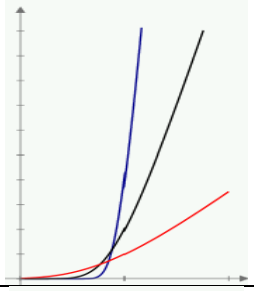
Exponential	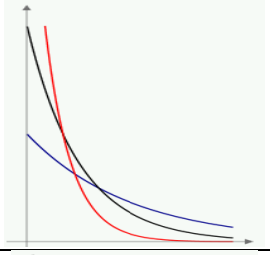	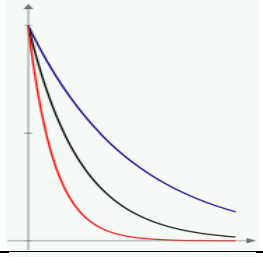	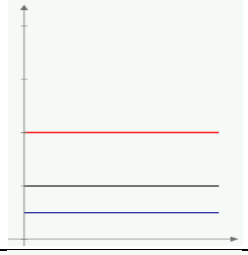
Lognormal	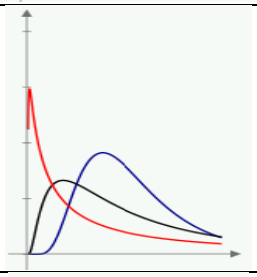	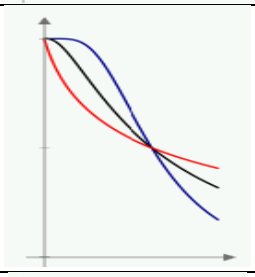	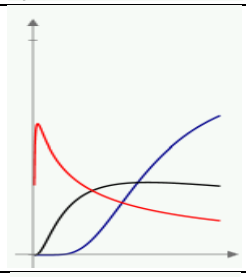
Weibull	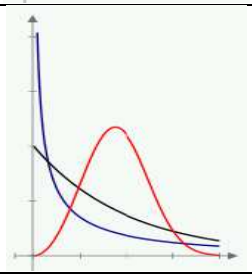	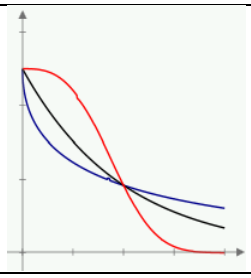	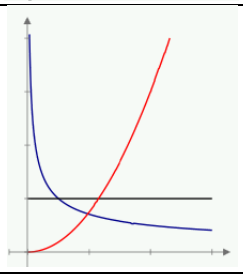

Figure IV.4: Life distribution functions represented schematically.

One can remark a series of multiplicative factors is assuming the effect of each stressor is counted independently. This appears to be somewhat of a contradiction because the effects are not really independent, so we express the failure rate $\lambda(x,y)$ from equation IV.1 to IV.3 as:

$$\lambda = \lambda_0 \cdot exp\left(\frac{E_a}{k \cdot T}\right) \cdot exp\left[-\frac{a_0 \cdot S_{Br1} \cdot x}{2 \cdot k \cdot T}\right] \cdot exp\left[-\frac{b_0 \cdot S_{Br2} \cdot y}{2 \cdot k \cdot T}\right] \cdot exp\left(\frac{-a_1}{2} \cdot S_{Br1} \cdot x\right) \cdot exp\left(\frac{-b_1}{2} \cdot S_{Br2} \cdot y\right) \quad \text{Eq. IV-69}$$

with

$$\lambda_0 = \frac{1}{k_0} = \left(1 - exp\left(-\frac{\Delta S^\circ}{k}\right)\right)^{-1} \quad \text{Eq. IV-70}$$

Comparing equation V.4 and V.9, we observe the π factors can be defined as:

a) the listed in [4] or [66]

$$\pi_{T,T_{REF}} = exp\left[\frac{E_a}{k}\left(\frac{1}{T_{REF}} - \frac{1}{T_{op}}\right)\right] \quad \text{Eq. IV-71}$$

$$\pi_{S_{1_{op}},S_{1_{REF}}} = exp\left[\frac{a_1}{2} \cdot S_{Br1} \cdot \left(x_{op} - x_{REF}\right)\right] \quad \text{Eq. IV-72}$$

$$\pi_{S_{2_{op}},S_{1_{REF}}} = exp\left[\frac{b_1}{2} \cdot S_{Br2} \cdot \left(y_{op} - y_{REF}\right)\right] \quad \text{Eq. IV-73}$$

b) the one's not considered in [4] or [66]

$$\pi_{S_{1op},S_{REF},T_{op},T_{REF}} = exp\left[\frac{a_0 \cdot S_{Br1}}{2 \cdot k}\left(\frac{x_{op}}{T_{op}} - \frac{x_{REF}}{T_{REF}}\right)\right] \quad \text{Eq. IV-74}$$

$$\pi_{S_{2op},S_{REF},T_{op},T_{REF}} = exp\left[\frac{b_0 \cdot S_{Br2}}{2 \cdot k}\left(\frac{y_{op}}{T_{op}} - \frac{y_{REF}}{T_{REF}}\right)\right] \quad \text{Eq. II-75}$$

From this, we observe the equivalence with actual Standards is uncomplete because of missing terms, those related to external stressors like environmental (vibration, mechanical, radiation, humidity, etc).

E. Sedyakin principle

It would be very useful if one could somehow convert a rather complicated dynamical stress pulse, over some time interval t_1–t_2, into a rectangular pulse effective stress which would produce an equivalent amount of material/device degradation over this same time interval t_1–t_2.

Sedyakin principle

Assuming an Accelerated Failure Time Model (AFT) (e.g. only the time scale is affected under stress), in both cases, accelerating factors (AF) can apply based on equ. III.19. Quality Standards define also the similar rate function models and related AF. In 1966, Sedyakin [19] formulated his famous physical principle in reliability which states that for two identical populations of units functioning under different stresses S_1 and S_2, two moment's t_1 and t_2 are equivalent if the probabilities of survival until these moments are equal. The Figure IV.3 show how this principle also relates to the resulting reliability function $R(t)$ for a population submitted to a step stress conditions (these can be generalized to a superposition of various stressors as temperature, voltage, etc).

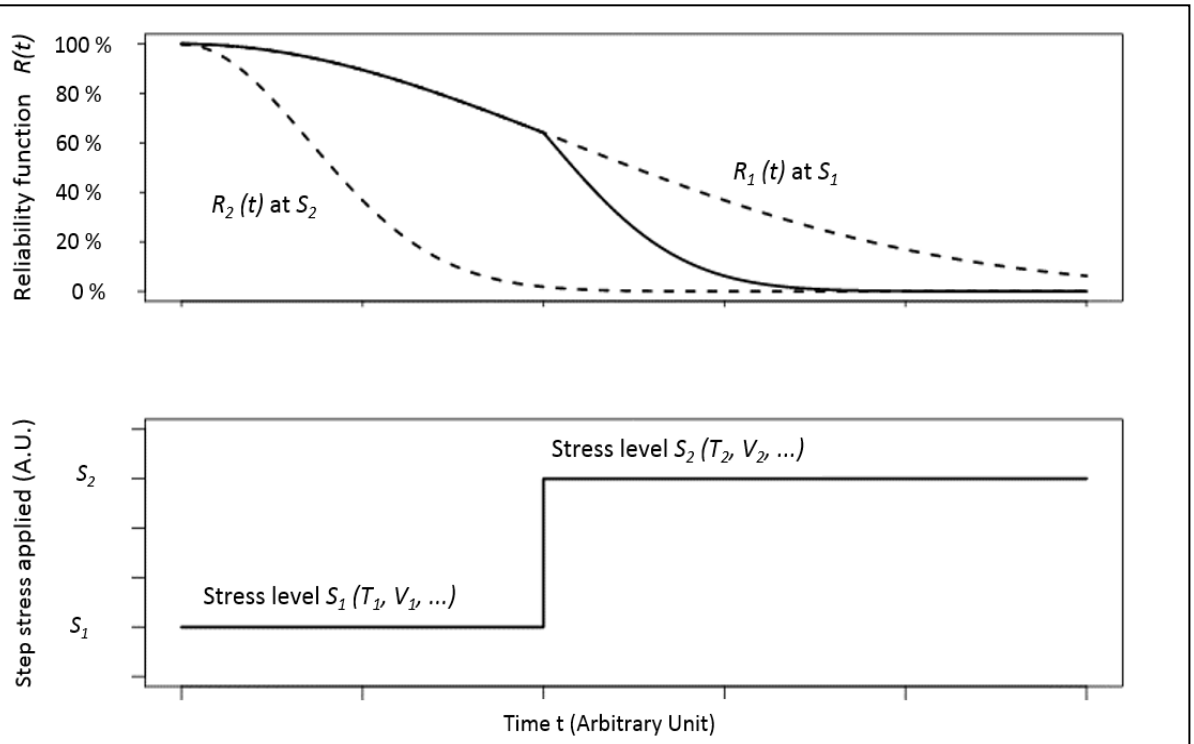

Figure IV.3: Reliability function $R(t)$ as a function of step stress applied and Sedyakin principle.

As presented by J. McPherson in ref [23] in his book chapter 14, and invoking potentially the Sedyakin principle, the time-to-failure models developed assume that the stress remains constant with time until the product fails. In semiconductor products (transistors, integrated circuits or any active electronic device) the applied signal induce voltage, current and power stresses changing during operation and are generally frequency dependent. So it is convenient to convert dynamical (time-dependent) stress to an equivalent effective static stress. So basic mathematics to determine the effective stress $\xi_{effective}$ such that it produce an equivalent amount of degradation and thus the same time-to-failure as the dynamical stress $\xi(t)$ is developed in ref [23] using the following concept of **compliance equation** for periodic (period P) dynamical stress and equivalent to power-law TF models :

$$\frac{1}{P} \cdot \int_0^P AF_{\xi(t),\xi_{effective}} \cdot dt = 1$$

Eq. II-76

Where the accelerating factor for the power-law TF model is for a yield stress $\xi_{yield} < \xi(t)$:

$$AF_{\xi(t),\xi_{effective}} = \left(\frac{\xi(t) - \xi_{yield}}{\xi_{effective} - \xi_{yield}} \right)^n$$

Eq. II-77

Gives:

$$\xi_{effective} - \xi_{yield} = \left[\frac{1}{P} \cdot \int_0^P \left(\xi(t) - \xi_{yield} \right)^n \cdot dt \right]^{\frac{1}{n}}$$

Eq. II-78

It is interesting to consider also how to calculate the effective static temperature equivalent proposed by J. McPherson. He mentioned that similar to stress, the temperature T of a device is not constant but depend on biasing on-off operation, pulse operation, thermal cycling, as well as on dynamic signal applied.

To assess the effective static temperature $T_{effective}$ which produces an equivalent amount of device degradation versus the temperature variation $T(t)$. The compliance equation to determine $T_{effective}$ over a time interval of ($t_a - t_b$)

$$\frac{1}{(t_a - t_b)} \cdot \int_0^P AF_{T(t),T_{effective}} \cdot dt = 1$$

Eq. II-79

III. SYSTEM RELIABILITY

A. *Series systems*

How to estimate the reliability distribution parameters and failure probabilities for complex DSM components operating at harsh condition as applied during their mission profiles?

The newest component technologies deploy transistors having very small gate lengths (less than 10 nm) with new materials, reduced dimensions, and new technologies. Once the emerging technologies for numerical applications under high environmental constraints for true and real-time mission profiles are validated, the issue is not yet completed.

In Part II, we have identified CMOS Bulk reliability distribution parameters accounting electrical aging mechanisms, such as high-temperature degradation so-called Negative or Positive Thermal Instability (NBTI, PBTI), or Hot Carriers Injection (HCI) and the hard or soft breakdown of dielectric gates. These mechanisms can cause significant reductions in performance and software errors that are very important to quantify under nominal operating conditions. We need to determine their impact on the lifetime of the single sensitive active area of a device and then to look on how it can degrade the performance of the design. It is important to note that most of these mechanisms do not directly lead to a straightforward failure but only a gradual parametric drift of the elementary functions which will only induce a failure when the parameters exceed a critical threshold strongly dependent on the architecture. For the dominant mechanisms in recent technologies, this failure rate increases over time, a characteristic property of Wearout mechanisms. Moreover, the reliability of the current circuits often leads to not observe any failure associated with these mechanisms for the duration of the tests (a few months), which does not make it possible to evaluate the probability of failure beyond the equivalent duration of the test, this probability being likely to increase strongly then because of the increasing nature of the failure rate.

How can these probabilities be used to predict total component DSM system performance? How does the DSM design affect reliability? How redundancy design in a DSM affect the total reliability?

What are the hypotheses to consider a system reliability model like a DSM?

How component failure rate characteristics are described: multiple failure mechanisms superimposed dependent or independent, constant (cataleptic failures) vs non-constant. What if a failure results in an open path or in a short circuit path and what could be such an impact for series or parallel system modelling?

This chapter will derive the formula for the reliability of a series system, parallel system or a mix series/parallel system as fully detailed in ref [67] in Applied Reliability Third Ed. book from P. Tobias and D. Trindade.

The most commonly used model for system reliability assumes that the system is made up of n independent components which all must operate in order for the system to function properly. But this series model is applied specifically when a single integrated circuit with several independent failure modes is analogous to a system with several independent elementary constituents. The failure mechanisms are competing with each other in the sense that the first to reach a failure states causes the component to fail: the open question is still to consider what a failure state is? Is it for catastrophic failure or related to a

failure criteria or performance? As argued by P. Tobias and D. Trindade, "*the more general competing risk model where the failure processes for different mechanisms are not independent can be very complicated since one must know how the random times of failure for different mechanisms are correlated*".

Assuming the first hypothesis, and the i[th] element have a cumulative distribution function (CDF) $F_i(t)$, the probability the serie system fails at time t is the probability that one or more of the n independent components have failed at time t. In term of total probability, we consider the product of the n CDFs:

$$R_s\,(t) = Pr(E) = \Pr(E_1, E_2, \dots, E_n) = \Pr(E_1) \cdot \Pr\,(E_2) \cdot \dots \cdot \Pr\,(E_n) = \prod_{i=1}^{n} R_i(t) \qquad \text{Eq. III-1}$$

With

$$R_i\,(t) = e^{-\lambda_i \cdot t} \qquad \text{Eq. III-2}$$

where λ_i is the failure rate of i^{th} component. Hence,

$$\lambda_s\,(t) = \sum_{i=1}^{n} \lambda_i \qquad \text{Eq. III-3}$$

If the components have the same reliability R_{s0}, meaning $\lambda_i = \lambda_0$ for i = 1 to n, this becomes:

$$R_s(t) = R_{s0}^n = \left(e^{-\lambda_0 \cdot t}\right)^n = e^{-n \cdot \lambda_0 \cdot t} \qquad \text{Eq. III-4}$$

LEMMA: A series system constituted of *n* identical and independent elements, each described by a POISSON distribution (λ_0) reliability model can be approximated by a general equivalent POISSON distribution with parameter $n \cdot \lambda_0$.

B. Parallel systems

A system that operate with n elements in parallel survives until the last of its element fails considering in this case a failure mode definition to be an open circuit. We will not consider the second hypothesis case if the failure mode of each element is a short circuit. In such a case the system with n elements in parallel survives if only one element fails.

Assuming the first hypothesis, and the i[th] element have a cumulative distribution function (CDF) $F_i(t)$, the probability the parallel system fails at time t is the probability that all the components have failed at time t. In term of total probability, we consider the product of the n CDFs:

$$F_p\,(t) = \prod_{i=1}^{n} F_i(t) \qquad \text{Eq. III-5}$$

$$R_p\,(t) = 1 - \prod_{i=1}^{n} [1 - R_i(t)] \qquad \text{Eq. III-6}$$

Poisson distribution function:

If the CDF is defined by Poisson or exponential distribution function, the probability the system fails, e.g. one at least of the n elements fails, is the reliability or probability of success at time *t*: as expressed by equation VII.3

$$R_p\,(t) = 1 - \prod_{i=1}^{n} \left(1 - e^{-\lambda_i \cdot t}\right) \qquad \text{Eq. III-7}$$

If $\lambda_i = \lambda$ for any i = 1 to n

$$R_p\,(t) = 1 - \left(1 - e^{-\lambda \cdot t}\right)^n \qquad \text{Eq. III-8}$$

Considering the life mission t is defined by the plateau of the bathtub, for $\lambda \cdot t << 1$, and we can approximate the reliability at time *t* by:

$$e^{-\lambda \cdot t} \approx 1 - \lambda \cdot t \qquad \text{or} \qquad \lambda \cdot t \approx 1 - e^{-\lambda \cdot t} \qquad \text{Eq. III-9}$$

and merging equ. VII.8 with VII.9 gives:

$$R_p(t) \approx 1-(\lambda\cdot t)^N \approx e^{-(\lambda\cdot t)^n} = e^{-\left(t/\theta\right)^\beta} \qquad \text{Eq. III-10}$$

The error generated by the approximation of equation VII.7 is assessed and plotted figure 4 showing equations VII.8 and VII.10 versus parameter $\lambda{\cdot}t$ in unit of MTTF. The error generated by the approximation is less than 1% for $\lambda\cdot t \leq 0.3$ or in other word at time *t* lower or equal to 30% of MTTF (for λ = 100 FIT and n=3, MTTF=1/λ = 10^7 hrs). This error is decreasing for higher values of n.

As a major fact, such parallel system on *n* independent and identical elements having the same constant Poisson failure rate λ (e.g. same equivalent $MTTF_i = MTTF = 1/\lambda$ for *i*=1 to *n*) show an equivalent Weibull distribution for short times t ≤ 30%·MTTF range for a error lower than 1%.

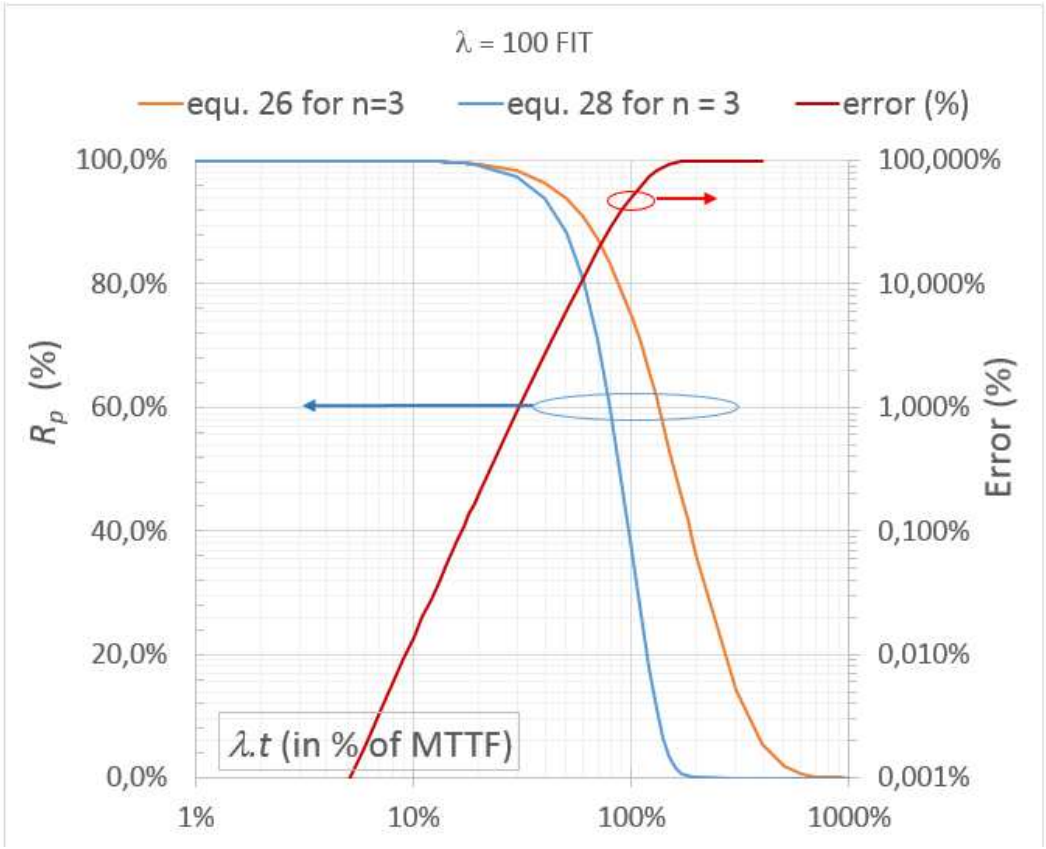

Figure V-6: Plot error (in red) as the difference between plot of equation VII.8 and VII.10 for λ=100FIT and *n*=3.

LEMMA: A parallel system constituted of *n* identical and independent elements, each described by a POISSON distribution (λ) reliability model can be approximated by a general equivalent WEIBULL distribution with parameters λ and $\beta = n$ with an error lower than 1% for time operation lower than 30%·MTTF for the example shown.

Weibull distribution function:

The random variable T has a Weibull distribution with parameters α_i and β_i if the reliability or probability of success at time *t* is given by:

$$R_{i_W}(t,\alpha_i,\beta_i) = e^{-\left(\frac{t}{\alpha_i}\right)^{\beta_i}} \quad , t \geq 0 \qquad \text{Eq. III-11}$$

$$R_{p_W}(t,\alpha_i,\beta_i) = 1-\prod_{i=1}^{n}\left(1-e^{-(\beta_i\cdot t^{\mu_i})}\right) \qquad \text{Eq. III-12}$$

For identical independent elements we set $\alpha_i = \alpha$ and $\beta_i = \beta$ for any *i* = 1 to *n*, so:

$$R_{p_W}(t,\alpha,\beta) = 1 - \left[1 - e^{-\left(\frac{t}{\alpha_i}\right)^{\beta_i}}\right]^n$$

Eq. III-13

Considering the life mission t is defined by the plateau of the bathtub, for $\lambda \cdot t << 1$, and we can get for a parallel system and short time t:

$$R_{p_W}(t,\alpha,\beta) \approx e^{-\left(t/\alpha\right)^{\beta \cdot n}}$$

Eq. III-14

The error generated by the approximation of equation VII.14 is assessed and plotted figure 5 showing equations VII.13 and VII.14 versus parameter $\lambda \cdot t$. The error generated by the approximation is less than 1% for $\lambda \cdot t \leq 0.3$ or in other word at time *t* lower or equal to 80% of MTTF (for example λ = 100 FIT and n=5). This error is decreasing for higher values of *n* and β.

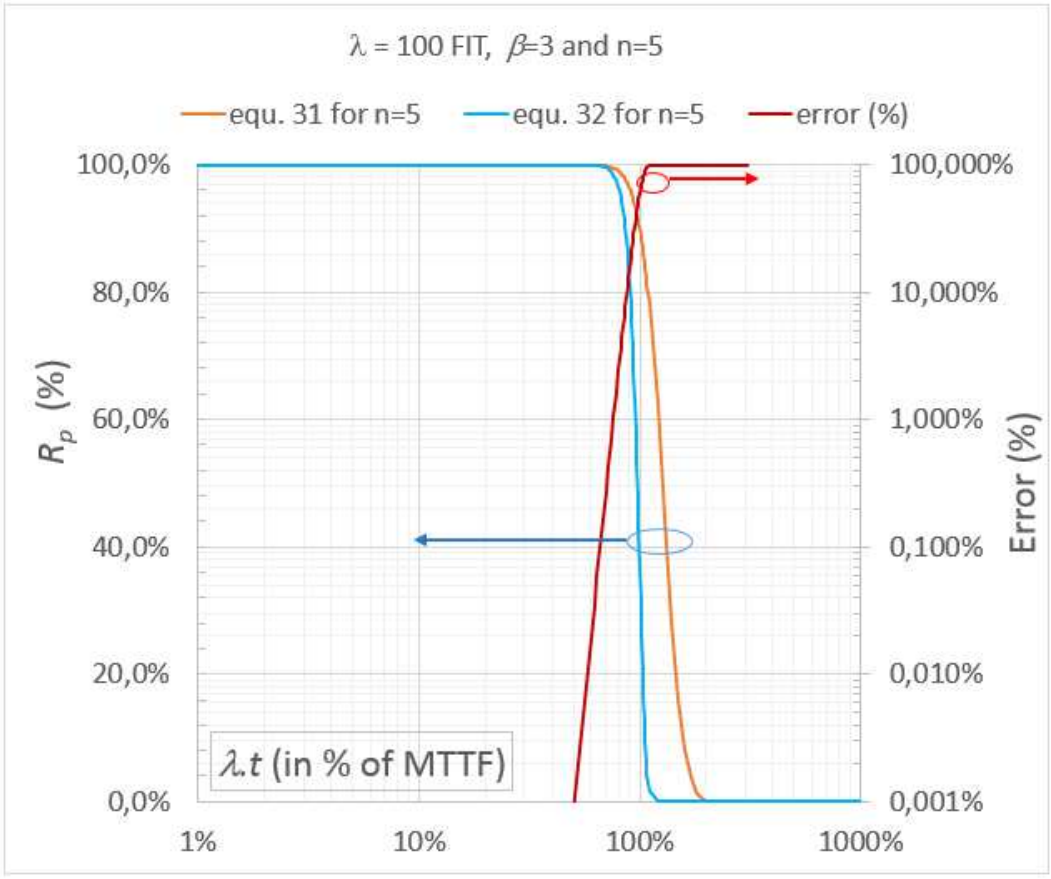

Figure V-7: Plot error (in red) as the difference between equation VII.13 and VII.14 for λ=100FIT, β=3 and

LEMMA: A parallel system constituted of *n* identical and independent elements, each described by a reliability WEIBULL distribution (α, β) model can be approximated by a general equivalent WEIBULL distribution with parameter (α, $\beta \cdot$ n) with an error lower than 1% for time operation lower than 75%· MTTF.

As a major fact and a generalisation point of view, such parallel system based on *n* independent and identical elements having the same constant Weibull failure rate parameters (α, β) is shown to be modelled by an equivalent Weibull distributions with reliability parameter (α, $\beta \cdot n$). The error induced by such approximation is estimated for short times t $\leq$ 80%· MTTF and range for an error lower than 1% for the example shown for λ=100FIT, β=5 and *n*=3.

C. Complex systems

Physical configurations in series or parallel do not necessarily indicate the same logic relations in terms of reliability. An integrated circuit (DSM) composed of LUTs connected in logical paths contains billions of elementary structures inter-connected. From a reliability perspective the LUT includes multiple transistors in series-parallel configurations but a LUT is said to have failed if one or more transistor failed. So, the transistors in a LUT are considered in series from a reliability perspective.

There are systems that require more than one component to succeed in order for the entire system to operate. In addition, the performance of a product is usually measured by multiple characteristics. In many applications, there is one critical characteristic, which describes the dominant degradation process. This one can be used to characterize product reliability. The failure of a product can be defined in terms of performance characteristic or called indicator crossing a specific threshold. Figure 6, depicts the relation of degradation path, pseudo-life, and life distribution. The maximum likelihood method should be used for estimation of distribution parameters. Once the estimates of reliability parameters we can use a Monte Carlo simulation to generate a large number of degradation paths. The probability of failure *F(t)* is approximated by the percentage of simulated degradation paths crossing a specified threshold after a stress time applied.

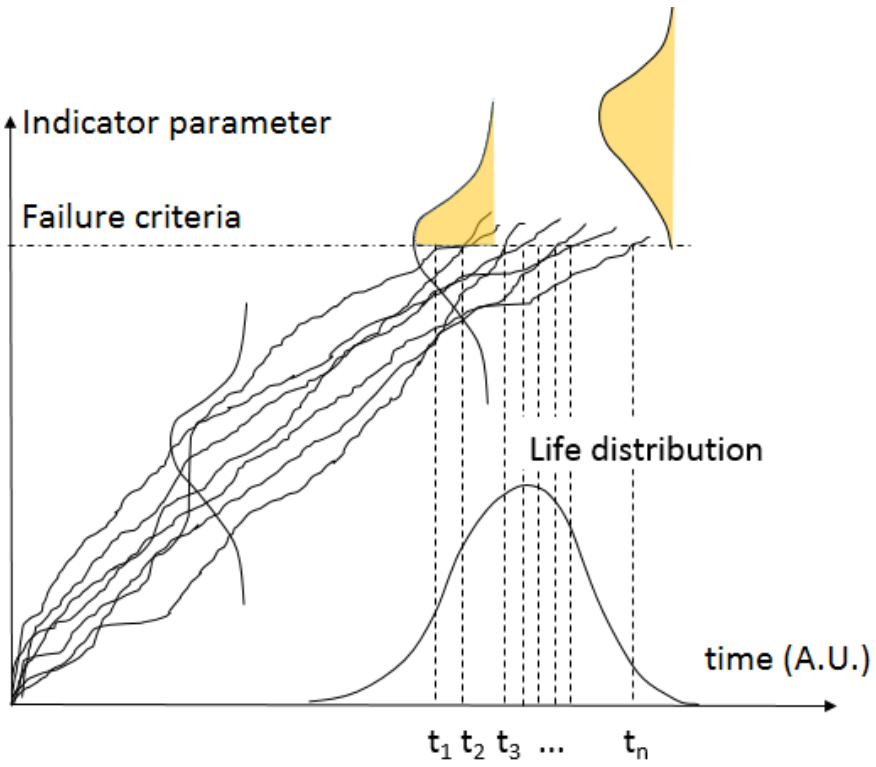

Figure V-8: Relation of degradation path, pseudo-life, and life distributions.

When considering catastrophic failure paradigm, a general series system can be observed in a configuration for a DSM FPGA test structure based on ring oscillator (RINGO) test structure represented in **Figure V-9**.

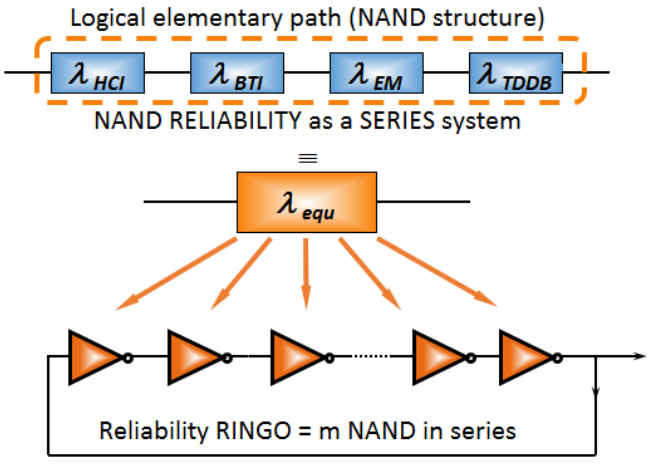

Figure V-9: Series reliability configuration for DSM RINGO catastrophic failure mode modelling. (4 failure mechanisms and m= RINGO size defined as number of NAND interconnected).

Nevertheless, if we consider parametric failure mechanisms hypothesis, another representation should be proposed as shown in **Figure V-9**. In such a case a single component with 4 independent parametric failure mechanisms (HCI, BIT, EM or TDDB) and occurring simultaneously, is analogous to a series system. Each failure mechanism 'competes' with the others to cause a failure and failure rates are additive, mechanism by mechanism, and so drifts are cumulated. In a RINGO structure, a failure is observed when all NAND fail in a cumulated drift failure reaching the failure criteria. In such a case, the reliability model is similar to a parallel system because by definition only the failure of all components within the system results in the failure of the entire system. In other words, we know a parallel system succeeds if one or more components are operational. Considering a parametric drift failure, the NANDs work together pending to reach the cumulated parameter drift limit and because the contribution of each failure mechanism is accumulated.

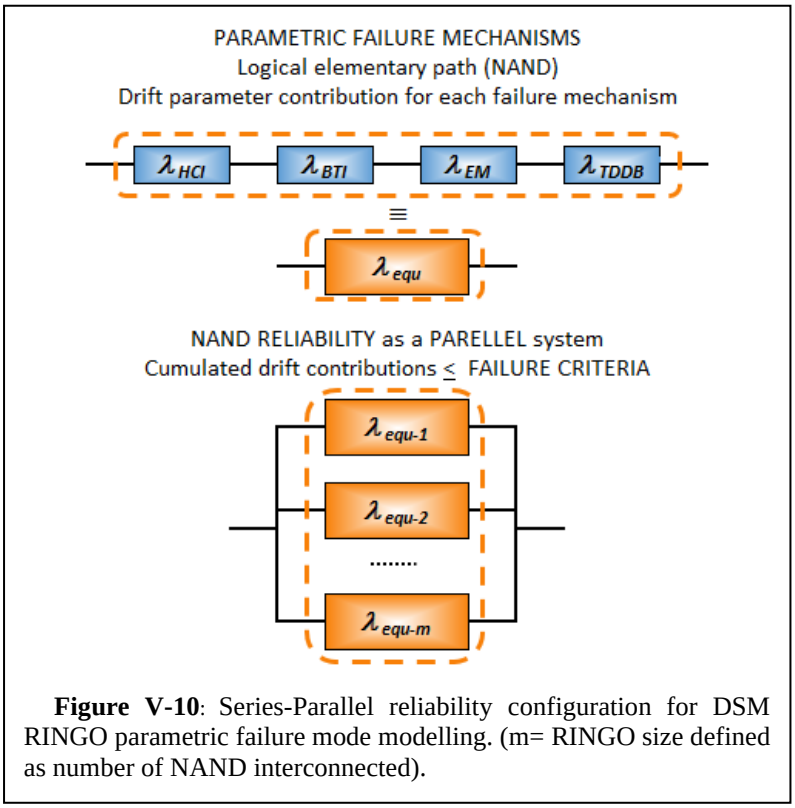

Figure V-10: Series-Parallel reliability configuration for DSM RINGO parametric failure mode modelling. (m= RINGO size defined as number of NAND interconnected).

A reliability of a series-parallel system defined in **Figure V-10** and for *a **POISSON distribution function,*** is written as:

$$R_{p-s_P}\left(t, \alpha_{i,j}, \beta_{i,j}\right) = 1 - \prod_{j=1}^{m}\left(1 - \prod_{i=1}^{4} e^{-\lambda_i \cdot t}\right) \quad \text{(Eq. 15)}$$

Considering *m* NAND elements in parallel each with 4 types of failure mechanisms in series, we get

$$R_{p-s_P}\left(t\right) = 1 - \prod_{j=1}^{m}\left(1 - e^{-t \cdot \sum_{i=1}^{4} \lambda_i}\right) \quad \text{(Eq. 16)}$$

Because all NAND elements are similar, we can write:

$$R_{p-s_P}\left(t\right) = 1 - \left[1 - e^{-t \cdot \sum_{i=1}^{4} \lambda_i}\right]^m \quad \text{(Eq. 17)}$$

If $\sum_{i=1}^{4} \lambda_i \cdot t << 1$, e.g. assuming true up to few percent's of MTTF, we can approximate the reliability at time *t* by:

$$\left(1 - e^{-\sum_{i=1}^{4} \lambda_i \cdot t}\right)^m \approx \left(t \cdot \sum_{i=1}^{4} \lambda_i\right)^m \quad \text{(Eq. 18)}$$

And (Eq**. 17** reduces to:

$$R_{p-s_P}\left(t\right) \approx 1 - \left(t \cdot \sum_{i=1}^{4} \lambda_i\right)^m \quad \text{(Eq. 19)}$$

Allowing us to express:

$$R_{p-s_P}(t) \approx 1 - \left(t \cdot \sum_{i=1}^{4} \lambda_i\right)^m \approx e^{-(t \cdot \Sigma_{i=1}^{4} \lambda_i)^m} = e^{-\left(t/\theta\right)^\beta} \quad \text{(Eq. 20)}$$

as a WEIBULL general equivalent representation where

$$\frac{1}{\theta} = \sum_{i=1}^{4} \lambda_i \quad \text{and} \quad \beta = \text{m} \quad \text{(Eq. 21)}$$

which is indeed the number of NANDs incorporated in a RINGO test structure.

LEMMA #04: In a series-parallel system constituted of *n* identical and independent elements, each described by a reliability POISSON distribution (λ), its reliability model can be approximated by a general equivalent WEIBULL distribution with parameter (θ, β= m) with an error lower than 3% for time operation lower than 50%·MTTF (see Figure V-11).

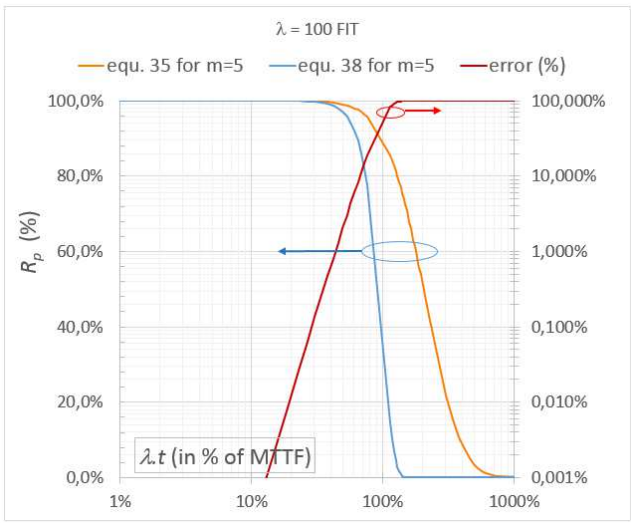

Figure V-11: Plot error (in red) as the difference between plot of Eq. 35 and Eq.38 for a POISSON Distribution with λ=100 FIT, β=m=5.

IV. CONCLUSION AND PROSPECTIVES

Using emerging microelectronic COTS appear mandatory to achieve today's product and system performances with the drawback of lack of inadequate Quality Standards which don't address in a proper manner the way to qualify them in a proper short period of time. Indeed, in the last end of XX^{th} century, the introduction of a new component in a Space system required few years of evaluation and complete qualification. Such timing was compatible with the technology evolution and the satellite development and manufacturing phases. Today, with the explosion of satellite constellation and their short development and production phase in less than 2 to 3 years, such Standards are not adapted in some case.

To balance this inconvenience, we need to better understand the physics of semiconductors and failure mechanisms in order to quickly identify and select "reliable COTS" technology and lot screening before to authorize their implementation in complex systems. By "reliable COTS" we consider we have enough information consolidated by short time adapted experiments to identify how we can guarantee mission profile as existing for Low Earth Orbit satellite (LEO) constellation or long-term Geostationary Earth Orbit telecommunication satellite. Same kind of considerations must be fixed based on skill and knowledge of Physics of devices to draw optimized experiments and deep analyses related to the Automotive or Aeronautic industries.

A reliability engineer team needs to gather multi-skills people having valuable knowledge on (not exhaustive):

- electronic design, to be able to understand how the devices are biased (DC and digital or analog signals) and stressed from normal to extreme mission profile conditions,
- semiconductor and assembly process manufacturing, characterization and metrology technics, to understand how devices are packaged and tested with the aim of determine and validate their Safe Operating Area limits and to define sequence of screening for efficient freak distributions purging, and their ability to survive operating life environmental and application conditions,
- physics of semiconductor, physics of new microelectronic device, induced failure mode and mechanisms to understand how devices are designed and manufactured so as to determine what are the key electrical stressors and indicators to monitor degradation patterns influenced by internal and external stress conditions (respectively biasing and environmental),
- reliability concepts and modelling, to identify and consolidate hypotheses of degradation based on series of experiments (as short as possible) representative of true mission conditions.

In the paradigm of Physics of Failure, people focus on how a product is failing either catastrophically or gradually.

In the Physics of Healthy we propose to focus on the characterization and physical reliability knowledge of lot devices able to assure the system mission in operation before failure. The goal is to provide advices to the equipment engineer on associated quality and reliability risks.

The very short development of new technologies into the custom market seized the microelectronic COTS products, and consequently induce a change in the technique high reliability application are designed.

This Part I is dedicated to understanding how PoH concept can be defined. To do so, we first focused to describe two kind of emerging technologies DSM (very narrow node size, e.g. < 10 nm and GaN Power DC switch transistor in a short State of The Art review. Letting aside the random failure of device, system or equipment breakdowns generally due to handling, packaging or external overstress, we concentrate on wearout mechanisms description taking advantage of J. McPherson's book on Reliability Physics and Engineering implementing the basics of reliability modelling [23], we presented and detailed the mathematics based on Gibbs Free Energy diagram considering reaction with several external stresses applied and temperature. The multi-failure mechanisms are also considered to elaborate a reliability model and to establish accelerating factor multi stress and multi-mechanism expression based on a non-constant activation energy.

Reliability models were also recalled with respect to random failure rate modelling and system reliability are presented from formula of series systems, parallel systems or a mix series/parallel system as fully detailed in book from P. Tobias and D. Trindade.

Establishing and reminding these preliminary set of mathematics, we propose to develop the next Part II to show how these tools can be applied and used experimentally to predict pre-failure occurrence and elaborate predictive reliability SHM protocols. A set of sequence is described to help to diagnostics PoH capability on new COTS devices through a series of control steps also named Prognostics and Health Management Protocol. Such protocol can be easily applied both on new emerging or existing technologies.

V. BIBLIOGRAPHY

[1] M. White and J. B. Bernstein, "Microelectronics Reliability: Physics-of-Failure Based Modeling and Lifetime Evaluation," *JPL Publication 08-5, Jet Propulsion Laboratory/California Institute of Technology,* February 2008.

[2] National Academy of Sciences, "Panel on Reliability Growth methods for Defense; Reliability Growth: Enhancing Defense System Reliability," The National Academies Press, Washington, DC. ISBN 978-0-309-31474-9, 2008.

[3] P. Lall, M. Pecht and E. B. Hakim, Influence of Temperature on Microelectronics and System Reliability, Boca Raton, NY: CRC Press, 1997.

[4] DoD, "MIL-HDBK-217, Military Handbook for Reliability prediction of Electronic Equipement," Washington, DC, USA, 1991, December.

[5] JEDEC, "JEDEC JEP-122G Failure Mechanisms and Models for Semiconductor Devices," JEDEC Solid State Technology Association, Arlington, 2011.

[6] J. B. Bernstein, M. Gabbay and O. Delly, "Reliability Matrix Solution to Multiple Mechanism Prediction," *Microelectronics Reliability Journal,* vol. 54, pp. 2951-2955, 2014.

[7] Robustness Group ZVEI, Handbook for Robustness Validation of Automotive Electrical/Electronic Modules, Frankfurt am Main, June 2013.

[8] QUANTERION, «Handbook of 217Plus Reliability Prediction Models,» *QUANTERION Solution Inc.,* 2015.

[9] T.S.Q.&R.publications, "http://www.triquint.com/shared/pubs/processes/Micro_Millimeter_Wave_Reliability_Overview.pdf," [Online].

[10] J. Berthon, D. Regis and G. Hubert, "Utilisation des composants DSM dans le contexte aéronautique.," in *19ème Congrés de Maitrise des Risques et Sûreté de Fonctionnement,* Dijon, 21-23 Oct. 2014.

[11] S. Arrhenius, "Arrhenius, Ueber den Einfluss des Atmosphärischen Kohlensäurengehalts auf die Temperatur der Erdoberfläche," *Proceedings of the Royal Swedish Academy of Science,* vol. 22, no. 1, 1896.

[12] L. Boltzmann, "Boltzmann, The Second Law of Thermodynamics. Populare Schriften," in *Essay 3, Address to a Formal Meeting of the Imperial Academy of Science,,* 1886.

[13] M. Evans and M. Polanyi, "Inertia and driving force of chemical reaction," *Faraday Society (London) Trans,* vol. 34, pp. 11-29, 1938.

[14] E. Wigner, "The transition state method," *Faraday Society (London) Trans,* vol. 34, pp. 29-41, 1938.

[15] S. Glasstone, K. J. Laider and H. Eyring, The theory of rate processs: the kinetics of chemical reaction, viscosity, diffusion and electrochemical phenomena., New York: Mc Graw-Hill, 1941.

[16] G. Hammond, "A correlation of Reaction Rates," *J. Am. Chem. Soc.,* vol. 77, pp. 334-338, 1955.

[17] R. Drenick, «Mathematical Aspects of the Reliability Problem,» *Journal of the Society for Industrial and Applied Mathematics,* vol. 8, n° %11, pp. 125-149, 1960.

[18] E. Snow, A. Grove, B. Deal and C. Sah, "Ion Transport Phenomena in Insulating Films," *J. Appl. Phys.,* vol. 36, p. 1664, 1965.

[19] N. Sedyakin, "On one physical principle in reliability theory (in Russian)," *Techn. Cybernetics,* pp. 80-87, 1966.

[20] D. Cox, "Regression Models and Life-Tables," *Journal of the Royal Statistical Society. Series B (Methodological), Vol. 34, No. 2. (1972), pp.,* vol. 34, no. 2, pp. 187-220, 1972.

[21] H. Eyring, S. Lin and S. Lin, Basic Chemical Kinetics, New York - Chichester - Brisbane - Toronto: John Willey & Sons, 1980.

[22] J. McPherson and D. Baglee, "Acceleration factors for thin gate oxide stressing," *Proc. 23rd Annual IEEE IRPS,* p. 1, 1985.

[23] J. W. McPherson, Reliability Physics and Engineering - Time-to-failure modeling; 3rd Edition, Plano (TX) USA: Springer Nature Switzerland AG, 2019.

[24] E. Suhir, "Probabilistic Design for Reliability," *ChipScale Reviews,* vol. 14, no. 6, 2010.

[25] E. Suhir, "Predicted Reliability of Aerospace Electronics: Application of Two Advanced Concepts," *IEEE Aerospace Conference,* 2-9 March 2013.

[26] D. Jin and J. Del Alamo, "Impact of high-power stress on dynamic On-resistance of high-volatge GaN HEMTs," *Microelectronics Reliability Journal,* vol. 52, pp. 2875-2879, 2012.

[27] G. Meneghesso, M. Meneghini, A. Tazzoli, N. Ronchi, A. Stocco, A. Chini and E. Zanoni, "Reliability issues of Gallium Nitride HEMTs," *International Journal of Microwave and Wireless Technologies,* vol. 2, no. 1, pp. 39-50, 2010.

[28] J. Stathis, S. Mahapatra and T. Grasser, "Controversial issues in negative bias temperature instability," *Microelectronics Reliability Journal,* vol. 81, pp. 244-251, 2018.

[29] J. Black, "Black, Electromigration - A brief survey and some recent results," *IEEE, Trans. Electron Devices*, Vols. ED-16, p. 388, 1969.

[30] "RDF 2000 (UTE C 80-810, IEC-62380-TR Ed.1)," [Online]. Available: http://www.ute-fr.com/La-normalisation/UTE-and-standardisation.

[31] SIEMENS AG, SN29500, Reliability and Quality Specifications Failure Rates of Components, Siemens Technical Liaison and Standardisation, 1986.

[32] V. Huard, F. Cacho and X. Federspiel, "Technology scaling and reliability challenges in the multicore era," *IRPS*, 16-18 April 2012.

[33] R. Quay, Gallium Nitride Electronics, Berlin Heidelberg: Springer Series in Materials Sciences, 2008.

[34] J. Bernstein and A. Bensoussan, "Reliability Prediction with MTOL, proposed to IEEE System Qualification for Reliability," *Transaction on Devices and Material Reliability (TDMR)*, 2016.

[35] INTEL, "VDSM Issues and Design Methodology," Intel Microelectronics Services, January 2002.

[36] C. Lee, B. Welch and W. Fleming, "Reliability of AuGe/Pt and AuGe/Ni ohmic contacts on GaAs," *Electronics Letters*, vol. 17, pp. 407-408, 1981.

[37] M. Delaney, T. Wiltsey, M. Chiang and K. Yu, "Reliability of 0.25µm GaAs MESFET MMIC Process: Results of Accelerated Lifetests and Hydrogen Exposure," in *GaAs Reliability Workshop*, Philadelphia, PA, USA, 1994.

[38] K. Decker, "GaAs MMIC Hydrogen Degradation Study," in *GaAs Reliability Workshop*, Philadelphia, PA, USA, 1994.

[39] A. Bensoussan, P. Coval, W. Roesch and T. Rubalcava, "Reliability of a GaAs MMIC process based on 0.5µm Au/Pd/Ti gate MESFETs," in *32nd Annual Proceeding Reliability Physics, IRPS*, San Jose (CA), April 1994.

[40] J. Scotten, "/forum/content/8022-lithovision-2019-semiconductor-technology-trends-their-impact-lithography.html," SemiWiki.com, 24 Feb 2019. [Online]. Available: https://www.semiwiki.com. [Accessed 28 Feb 2019].

[41] M. Lapedus, "/big-trouble-at-3nm/," Semiengineering.com, 21 June 2018. [Online]. Available: https://semiengineering.com. [Accessed 28 February 2019].

[42] T. Ueda, "Reliability issues in GaN and SiC power devices," in *IEEE International Reliability Physics Symposium (IRPS)*, Waikoloa, Hawaii, USA, 2014.

[43] M. Meneghini and et al., "Normally-off GaN-HEMTs with p-type gate: Off-state degradation, forward gate stress and ESD failure," *Microelectronics reliability Journal*, vol. 58, pp. 177-184, 2016.

[44] G. Meneghesso, G. Verzellesi, F. Danesin, F. Rampazzo, F. Zanon, M. Meneghini and E. Zanoni, "Reliability of GaN High-Electron-Mobility Transistors: State of the Art and Perspectives," *IEEE Transactions on device and materials reliability,*, vol. 8, no. 2, pp. 332-343, 2008.

[45] Y. Wu, C.-Y. Chen and J. Del Alamo, "Temperature-accelerated degradation of GaN HEMTs under high-power stress: activation energy of drain-current degradation.," in *JEDEC Solid State Technology Association*, 2014.

[46] S. Wamock and J. Del Alamo, "OFF-state TDDB in high-voltage GaN MIS-HEMTs," in *IEEE International Reliability Physics Symposium (IRPS)*, Monterey, CA, USA, 2017.

[47] A. Guo and J. Del Alamo, "Positive-bias temperature instability (PBTI) of GaN MOSFETs," in *IEEE International Reliability Physics Symposium*, Monterey, CA, USA, 2015.

[48] M. Meneghini, G. Meneghesso and E. Zanoni, Power GaN Devices - Materials, Applications and Reliability, Springer, Power Electronics and Power Systems, Series editors J. H. Chow, A. M. Stankovic, D. Hill., 2017.

[49] B. Agarwala and al., "Dependence of Electromigration-induced Failure Time on Length and Width of Aluminium Thin-Film Conductors," *J. Appl. Phys.*, vol. 41, p. 3954, 1970.

[50] JEDEC, "JESD22-A108 HTOL Temperature, bias, and operating life," July 2017. [Online]. Available: www.jedec.org.

[51] K. Decker, "GaAs MMIC Hydrogen Degradation Study," in *GaAs Reliability Workshop*, Philadelphia, PA, USA, 1994.

[52] S. Kayali, G. Ponchak and R. Shaw, "“GaAs MMIC Reliability Assurance Guidelines for Space Applications," JPL Publication, Vol 96-25, Pasadena, CA, 1996.

[53] M. Meneghini, G. Meneghesso and E. Zanoni, Power GaN Devices - Materials, Applications and Reliability, Springer, Power Electronics and Power Systems, Series editors J. H. Chow, A. M. Stankovic, D. Hill., 2017.

[54] G. Meneghesso, G. Verzellesi, F. Danesin, F. Rampazzo, F. Zanon, M. Meneghini and E. Zanoni, "Reliability of GaN High-Electron-Mobility Transistors: State of the Art and Perspectives," *IEEE TRANSACTIONS ON DEVICE AND MATERIALS RELIABILITY,*, vol. 8, no. 2, pp. 332-343, 2008.

[55] A. K. M. C. a. M. M. H. Yunm, "Entropic Approach to Measure Damage with Applications to Fatigue," *Annual Reliability and Maintainability Symposium (RAMS), Reno, NV,*, pp. 1-6, 2018.

[56] J. McPherson, R. Khamankar and A. Shanware, "Complementary model for intrinsic TDDB in SiO2 dielectrics," *J. Semiconductor Sci. Technol.*, vol. 15, p. 462, 2000.

[57] J. McPherson, "Stress dependent activation energy," *Proc. IEEE 24th IEEE IRPS*, p. 12, 1986.

[58] A. Bensoussan and E. Suhir, "Design-for-Reliability (DfR) of Aerospace Electronics: attributes and challenges," *IEEE Aerospace Conference*, 2-9 March 2013.

[59] S. Zhurkov, "Kinetic Concept of the Strength of Solids," *Int. J. of Fracture Mechanics*, vol. 1, no. 4, 1965.

[60] D. Cox and D. Oakes, Analysis of Survival Data, Volume 21 Chapman & Hall/CRC Monographs on Statistics & Applied Probability, CRC Press - 208 pages, 1984.

[61] J. W. PcPherson, ""Future of Reliability Testing - Can Zero Failures become reality"," in *ESREF 2019*, Toulouse, September 2019.

[62] L. Pierrat, «Estimation and validation of predictive reliability - Technical Report LJC-VAL/PTS,» VALEO Powertrain Thermal Systems (Internal report study) - LJ-CONSULTING, 2017.

[63] D. Delaux, «Fiablité Appliquée pour l'Industrie,» Valeo PTS (internal report), 2019.

[64] L. Pierrat et D. Delaux, «Analytical improvement of the Stress-Strength Method by considering a realistic strength distribution.,» chez *2013 ARS, Europe*, Berlin (Ge), 2013.

[65] E. Sperling, "https://semiengineering.com/gaps-emerge-in-automotive-test/," Semiconductor Engineering, 05 May 2019. [Online]. Available: https://semiengineering.com. [Accessed 08 May 2019].

[66] FIDES_Guide, "Reliability Methodology for Electronic Systems, DGA," 2004.

[67] P. A. Tobias and D. C. Trindade, Applied Reliability (3rd Ed.), Boca Raton, FL: CRC Press, 2012.